Mercury induces tight junction alterations and paracellular transport in colon epithelial cells through oxidative stress and thiol-redox dysregulation – Protection by novel lipid-soluble thiol antioxidant and heavy metal chelator, *N,N'*-bis-2-(mercaptoethyl)isophthalamide (NBMI)

Honors Research Thesis

Presented in Partial Fulfillment of the Requirements for graduation

"with Honors Research Distinction in Microbiology" in the College of Arts and Sciences

of The Ohio State University

by

Aarti Vala

The Ohio State University

June 2012

Project Advisor:

Narasimham Parinandi, Ph.D.

Dorothy M. Davis Heart & Lung Research Institute

Division of Pulmonary, Allergy, Critical Care, and Sleep Medicine, College of Medicine

The Ohio State University

Abstract

Intestinal permeability, characterized as leaky-gut syndrome, is a debilitating gastrointestinal disorder that leads to inflammation and altered immune response. Tight junctions are crucial for cell-to-cell adhesion and regulation of paracellular transport of molecules across the intestinal epithelium. However, the exact mechanism of the leaky-gut state encountered in autistic spectrum disorders is not known. Mercury, both as inorganic and organic forms, has been identified as a serious environmental pollutant, occupational hazard, and pharmaceutical toxicant. Mercury, in the form of thimerosal in vaccines, has been implicated as one of the causative species of autism. Therefore, here, we hypothesized that mercury would cause intestinal epithelial cell tight junction alterations and paracellular hyperpermeability (leak) through oxidative stress and thiol-redox dysregulation which could lead to the leaky-gut condition. Hence, we investigated the mechanism of tight junction alteration and paracellular leak of macromolecules in the well-established *in vitro* intestinal (colon) epithelial Caco-2 cell model. We also identified efficacy of the thiol-redox stabilization drugs to protect against the mercury-induced damage in the Caco-2 cells *in vitro*. Our studies revealed that the two forms of mercury, methylmercury and thimerosal caused (*i*) dose- and time-dependent cytotoxicity (lactate dehydrogenase release, decreased mitochondrial integrity, and cell morphological alterations), (*ii*) loss of intracellular glutathione (GSH), (*iii*) increase in the formation of reactive oxygen species, (*iv*) loss of barrier dysfunction; (*v*) loss of cell proliferation, (*vi)* actin cytoskeletal rearrangement (actin stress fiber formation), (*vii*) tight-junction (ZO-1 protein and occludins) alterations, and (*viii*) increase in paracellular leak of macromolecules in Caco-2 cells *in vitro*. Mercury-induced cytotoxicity, tight junction

alterations, and increase in paracellular leak were significantly attenuated by the novel lipophilic thiol-redox-stabilizing antioxidant and heavy metal chelator, *N,N'*-bis-(2-mercaptoethyl)isophthalamide (NBMI). For the first time, the results of the current study demonstrated that mercury (methylmercury and thimerosal) caused intestinal epithelial cell damage and macromolecule leak through thiol-redox dysregulation and oxidative stress which was effectively protected by the novel lipophilic thiol-redox stabilizer and heavy metal chelator, NBMI. Our findings emphasize the significance of altered cellular functioning by the intestinal epithelium upon exposure to mercuric agents, and pharmacological attenuation by the novel drug, NBMI.

Acknowledgments

I am thankful to my honors research project advisor and mentor, Dr. Narasimham Parinandi for guiding me throughout the project to completion and offering me an opportunity to conduct laboratory research.

I also thank my friends and co-researchers in the laboratory Dr. Sainath Kotha, Travis Gurney, Jordan Secor, Susie Butler, and Jamie Abbott and rest of the Parinandi Lab for the encouragement and unconditional support throughout our pursuit in the laboratory.

I thank Dr. Boyd Haley, Professor Emeritus, Department of Chemistry, University of Kentucky, Lexington, for providing NBMI for my research.

I extend my sincere appreciation to the Division of Pulmonary, Allergy, Critical Care, and Sleep Medicine and the Dorothy M. Davis Heart and Lung Research Institute for the opportunity to conduct my research.

Last but not the least, I sincerely thank my committee members, Dr. Tom Hund and Dr. Mahmood Khan for taking time amidst their busy schedules to adjudicate my dissertation.

Table of Contents

List of Figures

Introduction

Mercury is a prevalent environmental toxin that poses significant health concerns to humans and the environment. Mercury enters the environment and life forms including humans as inorganic form (metallic mercury vapor), organic mercury form (e.g. methylmercury), and pharmaceutical form (e.g. thimerosal). Sources of human exposure to mercury vary widely but include consumption of contaminated fish, exposure to power plant emissions, inoculation with vaccines preserved with the mercury containing thimerosal, and leeching from dental amalgams. Occupational and environmental exposure to mercury and other toxic metals including chromium, cadmium, and lead increase one's risk of heavy metal poisoning. Ingestion and inhalation of mercury and other heavy metals can result in many chronic and/or acute physiologic conditions. Specifically, mercury poisoning can result in upper respiratory tract diseases, lung diseases, cardiovascular disease, musculoskeletal disorders, and nervous system diseases including neurodegeneration.

The biomethylation of inorganic mercury by microorganisms leads to the formation of methylmercury, an organic and more toxic form of mercury (Dopp et al. 2011). Exposure to the organic form of mercury poses a greater risk to human health. Humans' consumption of contaminated fish is a primary mode of exposure to methylmercury. Many industrial processes result in contamination of marine environments, allowing aquatic bacteria to convert less hazardous inorganic mercury to the more toxic organic form. Consequently, both freshwater and saltwater fish have shown to be contaminated with methylmercury. When consumed by humans, mercury-contaminated fish are a source of mercury poisoning and a causative agent in human

disease. Therefore, exposure to methylmercury is a significant public health concern that warrants further investigation including examination of the cellular mechanism(s) of toxicity which are poorly understood.

In addition to the aforementioned adverse health effects, mercury has been implicated as a contributor to leaky-gut syndrome, or intestinal hyperpermeability. Leaky-gut syndrome is a condition in which alterations within the gastrointestinal epithelium compromise the guts selectively permeable luminal membrane. Specifically, disruptions in the essential intercellular tight junctions, which are mediated by ZO-1 and occludin proteins, facilitate dysregulated migration of bacteria, nutrients, and macromolecules. Such disruptions of intestinal barrier function and lack of epithelial junction integrity has been implicated as a causative agent of autoimmune and inflammatory diseases (Groschwitz & Hogan et al. 2009). However, the mechanisms by which mercury may contribute to process in not know.

Earlier, we reported that mercury induced toxicity in endothelial cells through generation of ROS and thiol-redox destabilization (Secor, et al.). However, the complete cellular mechanisms of mercury toxicity remain unclear and the effects on the gastrointestinal tract, specifically colonic epithelium, remain uninvestigated. The colonic epithelium is a monolayer lining the interior of the small and large intestines and is important for gastrointestinal function and health. The intestinal epithelium forms a barrier that separates the gastrointestinal lumen from the basolateral membrane and underlying capillary bed. Additionally, the intestinal epithelium is an integral regulator of digestion and facilitator of absorption which regulates transmigration. The structural integrity of this membrane is conferred in large part by the tight junctions between

intestinal epithelial cells. Tight junctions, while preventing invasion by enteric bacteria, do not form impermeable seals but allow paracellular absorption of essential nutrients. The functional importance of a dynamic, selectively permeable layer of cells (e.g. epithelial cells of the intestine) is mediated by the architecture of cytoskeleton proteins which compose tight junctions. Studies have shown that the tight junction barrier is highly-regulated and is modulated by actin cytoskeletal arrangement (Shen & Turner et al. 2006). Disruption of the intestinal epithelium through alteration of the actin cytoskeleton results in the intestinal hyperpermeability disorders and leaky-gut syndrome.

Consequently, here we hypothesized that mercury exposure compromises the structural integrity of the intestinal epithelium by causing cytotoxicity in intestinal epithelial cells through generation of ROS, disruption of tight junctions, and induction of cytoskeletal rearrangements which contribute to leaky-gut syndrome. Moreover, the leaky-gut syndrome is also encountered among autistic spectrum disorders. Therefore, here we tested our hypothesis by using our established intestinal Caco-2 colon epithelial cell model to investigate the cytotoxicity of mercury (as methylmercury and thimerosal). We assayed cytotoxicity using lactate dehydrogenase (LDH) release, MTT reduction (mitochondrial function), and cellular proliferation. We also measured changes due to mercury in intracellular glutathione (GSH) and ROS. Lastly, we indexed the effects of mercury on membrane integrity through determining trans-epithelial electrical resistance (TEpR) and macromolecule (FITC-dextran) leak across the paracellular gaps. For the first time, this study demonstrated a time- and dose-dependent cytotoxic effect of mercury on the colon epithelial cells. Furthermore, we demonstrated that mercury acted through depleting intracellular thiols (glutathione, GSH) and generation ROS which led to

cytoskeletal rearrangements and membrane dysfunction and, ultimately, cytotoxicity and paracellular hyperpermeability. Lastly, we report that the novel lipophilic thiol-redox stabilizing antioxidant and heavy metal chelator, *N*,*N*'-bis-(2-mercaptoethyl)isophthalamide (NBMI), attenuated the mercury-induced cytotoxicity, cytoskeletal rearrangement, tight junction alterations, and paracellular hyperpermeability by inhibiting the generation of ROS and preventing loss of intracellular thiols.

MATERIALS AND METHODS

Materials

Caco-2 cells used in this study, 1X trypsin-EDTA solution, Penicillin-Streptomycin solution, and Eagle's Minimum Essential Medium (EMEM) were obtained from ATCC (Manassas, VA). Phosphate-buffered saline (PBS) was obtained from Biofluids Inc. (Rockville, MD). Minimal essential medium (MEM), nonessential amino acids, fetal bovine serum (FBS), tissue culture reagents, meso-2,3-dimercaptosuccinic acid (DMSA), N-acetyl-L-cysteine (NAC), 3-[4,5-Dimethylthiazol-2-yl]-2, 5-diphenyl tetrazolium bromide reduction kit (MTT assay kit), lactate dehydrogenase cytotoxicity assay kit (LDH release assay kit), t-octylphenoxypolyethoxyethanol (Triton X-100), bovine serum albumin (BSA), and analytical reagents of highest purity were all purchased from Sigma Chemical Co. (St. Louis, MO). PD98059 was obtained from Calbiochem (San Diego, CA). Anti-rabbit AlexaFluor 488-conjugated antibody was purchased from Molecular Probes Invitrogen Co. (Carlsbad, CA). GSH chemiluminescence assay kit (GSH-Glo) was obtained from Promega Corporation (Madison, WI). [^{3}H]-Thymidine was obtained from American Radiolabeled Chemicals, Inc. (St. Louis, MO). ECIS electrode arrays were obtained from Applied Biophysics (Troy, NY). Paraformaldehyde was purchased from Electron Microscopy Sciences (Fort Washington, PA). Mouse anti-ZO1, anti-occludin antibody was obtained from Zymed Laboratories (San Francisco, CA). Polyoxyethylene sorbitan monolaurate (Tween-20) was purchased from Bio-Rad Laboratories (Hercules, CA).

NBMI Synthesis

NBMI was synthesized using a modification of the method of Matlocket al. (2003) at the University of Kentucky by Gupta under the supervision of Haley. Three grams of 2-aminoethylthiol hydrochloride was dissolved in 25 ml of chloroform and 3.7 ml of triethylamine and placed in an ice bath with stirring. A total of 2.68 g of isophthaloyl chloride was dissolved in 25 ml of chloroform and slowly added to the solution containing 2-aminoethylthiol and allowed to stir for 2 h on ice. A precipitation of the NBMI was induced by adding about 100 ml of 0.1 N HCl slowly to the stirring mixture. The resulting precipitate was collected by filtration and washed two times with a water:chloroform (50/50) mixture and then two times with 0.1 N HCl and three times with distilled water. The resulting white powder was dried under vacuum and yielded the product NBMI in 70% yield. Gram amounts of this powder were dissolved in pure ethanol and recrystallized twice resulting in the final product. NBMI purity was determined by LC-MS/MS. Column was a Waters X-Bridge C-18 (150 × 3.0 mm, 5 μm particle size). The mobile phase consisted of (A) aqueous with 0.1% formic acid and (B) methanol with 0.1% formic acid. A gradient system was used, and the total run time was 30 min. The elution conditions expressed as % of B is as follows: 0–30 s 10% B, 30 s–10 min 10–90% B, 10–19 min 90% B, 19–20 min 90–10% B, and 20–30 min 10% B. Injection volume was 10 μl. Flow rate was 250 μl/min and the retention time for NBMI was 9.81 min. Analysis was done on a Varian LC 1200 L Triple Quadruple MS, using a positive electro-spray ionization source.

Cell Culture

Caco-2 cells were cultured in EMEM supplemented with 20% (vol/vol) fetal bovine serum, 100 units/ml penicillin and streptomycin, and 1% (vol/vol) non-essential amino acids at 37^{o}C under a humidified 95% air - 5% CO_2 atmosphere. Cells in culture were maintained at 37ºC in a humidified environment of 95% air - 5% CO_2 and grown to contact-inhibited monolayers with typical cobblestone morphology. When confluence was reached, cells were trypsinized and subcultured in T 75-cm^2 flasks or 35 X 10-mm or 100-mm tissue culture dishes. Confluent cells showed cobblestone morphology under light microscope. All experiments were conducted between 8 and 30 passages (80-90% confluence). All media and treatments were carefully adjusted to pH 7.4 before use.

Lactate Dehydrogenase (LDH) Release Assay for Cytotoxicity

Cytotoxicity in Caco-2 cells was determined by assaying the extent of release of LDH from cells according to our previously published method (Patel et al., 2011). At the end of treatment, the medium was collected and LDH released into the medium was determined spectrophotometrically by using the commercial LDH assay kit according to the manufacturer's recommendations (Sigma Chemical Co., St. Louis, MO).

MTT Reduction Assay for Cytotoxicity

Cytotoxicity in Caco-2 cells was determined by assaying the extent of reduction of MTT in intact cells by using the commercial MTT reduction assay kit as previously shown (Sliman et al., 2009). At the end of the experimental treatments, MTT solution (10% by vol in MEM) was added and the cells were incubated for 3 h, following which MTT solvent was added in an amount equal to the original culture volume. Absorbance

of the reduced MTT was determined spectrophotometrically according to the manufacturer's recommendations (Sigma Chemical Co., St. Louis, MO).

Morphology Assay of Cytotoxicity

Morphological alterations in Caco-2 cells cultured in 35-mm dishes up to 70% confluence, following their exposure to mercury and other pharmacological treatments for 1 and 2 h, were examined as an index of cytotoxicity according to our previously established method (Mazerik et al. 2007). Images of cell morphology were digitally captured with the Olympus microscope at 20x magnification.

[^{3}H]-Thymidine incorporation assay for cell proliferation

Caco-2 cells were grown to 60% confluence in 35-mm dishes. Complete medium was removed from the culture dishes and the treatment solutions were added to the dishes. The treatment medium was then removed and 1 ml of [^{3}H]-thymidine (1 μCi/ml) in MEM was added to each well and incubated for 24 h. After incubations, [^{3}H]-thymidine was removed and cells were washed twice with ice-cold PBS. Cells were then washed twice with 5% trichloroacetic acid (TCA) in distilled water. Washings of 5% TCA were then removed and the cells were treated with 10.25 M NaOH (500 μL) for 30 min to solubilize the cells. The solubilized cell solution (400 μL) was transferred to the scintillation vials followed by the addition of 10 mL of scintillation cocktail, and then the [^{3}H] radioactivity was counted in the Packard Tri-carb 2900TR liquid scintillation counter.

Measurement of Transepithelial Cell Electrical Resistance

The transepithelial cell electrical resistance (TEpR) was measured according to our previously published method (Sliman et al. 2010). Caco-2 cells were cultured up to 90% confluence in complete MEM on gold electrodes (Applied Biophysics Inc., Troy, NY) under a humidified atmosphere of 95% air - 5% CO_2 at 37°C. The EC monolayers were then treated with MEM alone or MEM containing the desired concentrations of the pharmacological agents for 2 h. TEPCR of the monolayers was continuously measured on ECIS (Applied Biophysics Inc., Troy, NY) following the treatment of cells with MEM containing methylmercury (10 μM) or thimerosal (25 μM) under a humidified atmosphere of 95% air - 5% CO_2 at 37°C.

GSH Determination

Intracellular soluble thiol (GSH) levels were determined using the GSH-Glo GSH assay kit as reported earlier (Patel et al., 2011). Caco-2 cells grown up to 90% confluence in 96 well plates were treated with MEM alone or MEM containing desired concentrations of treatments under a humidified 95% air - 5% CO_2 atmosphere. Following incubation, intracellular GSH levels were determined according to the manufacturer's recommendations (Promega Corp. Madison, WI).

Measurement of Paracellular Epithelial Permeability

Caco-2 cells were grown to 80% confluence in 12-well Corning 3.0 μm pore-size culture inserts (Lowell, MA). The epithelial cell monolayers were treated with MEM alone or MEM containing selected pharmacological agents and methylmercury (10 μM)

or thimerosal (25 μM) for 2 h under a humidified atmosphere of 95% air - 5% CO_2 at 37°C. Following treatments, FITC-dextran (30 kDa) dissolved in phenol-free MEM was placed on the apical side of the monolayer, in the insert, and the cells were then incubated for 1 h under a humidified atmosphere of 95% air - 5% CO_2 at 37°C. The fluorescence of the FITC-dextran that leaked through the paracellular gaps of the EC monolayer was measured on a Bio-Tex ELx808 fluorescent plate reader set at 480 nm excitation and 540 nm emission, using appropriate blanks. The extent of FITC-dextran found in the basal side of the EC monolayer was expressed as arbitrary fluorescence units.

Reactive Oxygen Species Measurement by 2'-7'-Dichlorofluorescin Diacetate Fluorescence

Formation of ROS in Caco-2 cells in 35-mm dishes ($5x10^5$cells/dish) was determined by 20-70-dichlorofluorescin diacetate (DCFDA) fluorescence in cells preloaded with 10mmol/L DCFDA for 30 min in complete MEM at 37C in a 95% air and 5% CO2 environment prior to experimental treatments, according to our previously published procedure. 2'-7'-Dichlorofluorescin diacetate fluorescence as an index of intracellular ROS generation was visualized under Olympus fluorescence microscope at 50X magnification with excitation and emission set at 490 and 530 nm, respectively. Intracellular ROS formation was quantified by measuring DCFDA fluorescence in lysates of cells on a Bio-Tex ELx808 fluorescent plate reader set at 490 nm excitation and 530 nm emission, using appropriate blanks. The extent of intracellular ROS formation was expressed as the arbitrary fluorescence units.

Fluorescence microscopy of actin stress fibers

Formation of actin stress fibers, as an index of epithelial cytoskeletal reorganization, was examined by fluorescence microscopy according to our previously published method (Sliman et al., 2010). Caco-2 cells cultured on sterile coverslips (Harvard Apparatus, 22 mm2) in 35-mm sterile dishes at a density of 104 cells/dish were treated with MEM alone, MEM containing desired concentrations of mercury, or MEM containing selected pharmacological agents and desired concentrations of mercury for 30 min under a humidified atmosphere of 95% air - 5% CO_2 at 37°C. At the end of the incubation period, cells cultured on coverslips were washed with 1x PBS, fixed with 3.7% of paraformaldehyde for 10 min, permeabilized with 0.25% Triton X-100 in TBST containing 0.01% Tween-20 for 5 min, and blocked for 30 min with 1% BSA in 0.01% TBST. Actin stress fibers were visualized by staining the cells with rhodamine-phalloidin (1:50 dilution) in 1% BSA in TBST for 1 h. The cells were then washed four times with PBS, stained with 1% DAPI in PBS for 5 min, washed four times with PBS, mounted, and examined under Zeiss LSM 510 Confocal/Multiphoton Microscope at 543 nm excitation and 565 nm emission under 63x magnification. The images were captured digitally. The extent of the fluorescence intensity was measured using the Scion Image software.

Immunofluorescence microscopy of tight junction proteins

Caco-2 cells cultured on sterile coverslips (Harvard Apparatus, 22 mm2) in 35-mm sterile dishes at a density of 104 cells/dish were treated with MEM alone or MEM containing desired concentrations of mercury or MEM containing selected

pharmacological agents and desired concentrations of mercury for 30 min under a humidified atmosphere of 95% air - 5% CO_2 at 37°C. At the end of the incubation period, cells cultured on coverslips were washed with PBS, fixed with 3.7% of paraformaldehyde for 10 min, permeabilized with 0.25% Triton X-100 in Tris-buffered saline Tween-20 (TBST) containing 0.01% Tween-20 for 5 min, blocked for 30 min with 1% BSA in 0.01% TBST, and then incubated for 12 h at room temperature with mouse primary anti-occludin and anti-ZO-1 antibodies at a dilution of 1:200 (vol/vol) for the visualization of tight junction protein localized on the cellular membrane. Following the treatment of cells with the primary antibody, the cells were incubated with secondary anti-mouse AlexaFluor 488-conjugated antibody (1:100 dilution, vol/vol) for 1 h at room temperature. The coverslips with cells were then mounted on a glass slide with the antifade mounting medium, Fluoromount-G, and viewed with Ziess Confocal microscope at 63x magnification. The pictures were captured digitally, and the fluorescence intensity was quantified using the Scion Image software.

Statistical Analysis

All experiments were done in triplicate. Data were expressed as mean ± standard deviation (SD). Statistical analysis was carried out by ANOVA using SigmaStat (Jandel). The level of statistical significance was taken as $P < 0.05$.

RESULTS

Mercury induces cytotoxicity in colonic epithelial cells

In earlier studies, we reported that mercury induced cytotoxicity in bovine pulmonary artery endothelial cells (BPAECs) (REF). However, the effect of mercury treatment on Caco-2 cells is not known. With this data in consideration and as the first step in testing our hypothesis, we set out to determine whether mercury (as methylmercury or thimerosal) would cause cytotoxicity in our Caco-2 model. To determine this possibility, Caco-2 cells were treated with methylmercury (1, 5, and 10 μM) and thimerosal (5, 10, and 25 μM) for 1 and 2 h. Following treatment, lactate dehydrogenase (LDH) release and MTT reduction were measured as indices of cytotoxicity. Methylmercury and thimerosal caused significant time- and dose-dependent increases in LDH release in Caco-2 cells relative to untreated control cells (Figure 2A and B, respectively). Furthermore, methylmercury and thimerosal caused significant time- and dose-dependent decreases in MTT reduction in Caco-2 cells relative to untreated control cells (Figure 2C and D, respectively). These data revealed that mercury, as both methylmercury and thimerosal, caused significant time-and-dose dependent cytotoxicity in Caco-2 cells.

Thiol-redox stabilizing drug, NBMI, attenuates mercury-induced cytotoxicity in colonic epithelial cells

Previously, we have demonstrated that mercury-induced cytotoxicity in BPAECs was attenuated by the thiol-redox stabilizing drug, NBMI. Accordingly, we next examined the possibility that mercury-induced cytotoxicity in Caco-2 cells may occur

through thiol-redox destabilization and evaluated the effectiveness of NBMI in attenuating mercury-induced cytotoxicity in our colonic epithelial model. Caco-2 cells were pre-treated with NBMI (10, 25, and 50 μM) for 1 h prior to treatment with methylmercury (10 μM) and thimerosal (25 μM) for 1 h and LDH release and MTT reduction were measured following treatment as indices of cytotoxicity. In a significant dose-dependent fashion, NBMI attenuated mercury-induced increases in LDH release and MTT in Caco-2 cells (Figure 3). These results revealed that mercury-induced cytotoxicity in Caco-2 cells likely occurs through thiol-redox destabilization and NBMI is effective in attenuating mercury-induced cytotoxicity.

NBMI attenuates mercury-induced cytotoxicity with greater efficacy than well-established thiol-protectant antioxidants in colonic epithelial cells

After observing that NBMI attenuated mercury-induced cytotoxicity in Caco-2 cells, we next sought to compare the efficacy of NBMI to well-established thiol-redox stabilizing antioxidants in attenuating mercury-induced cytotoxicity. Specifically, we used the widely popular drugs N-acetlycysteine (NAC) and dimercaptosuccinic acid (DMSA) in our comparative analysis. Caco-2 cells were pre-treated with NBMI (50 μM), NAC (50 μM), and DMSA (50 μM) for 1 h prior to treatment with methylmercury (10 μM) and thimerosal (25 μM) for 1 h. Following treatment, LDH release was measured as an index of cytotoxicity. NBMI-treated Caco-2 cells demonstrated significantly less LDH release when compared to cells treated with methylmercury and thimerosal alone (Figure 4). Furthermore, the NBMI attenuation of mercury-induced LDH release was significantly greater than the attenuation exhibited by NAC and DMSA pre-treated Caco-

2 cells. Consequently, this experiment revealed that NBMI attenuated mercury-induced cytotoxicity with significantly greater efficacy than the well-established thiol-protectant antioxidant drugs, NAC and DMSA.

Mercury causes alterations in cell morphology of colon epithelial cells

Earlier studies have shown that mercury-induced cytotoxicity is associated with alterations in cellular morphology. As further investigation of mercury-induced cytotoxicity, we studied whether cellular morphology of Caco-2 cells would be altered after treatment with mercury. To determine this possibility, Caco-2 cells were treated with methylmercury (1, 5, and 10 μM) and thimerosal (5, 10, and 25 μM) for 1 h. Following treatment, we digitally captured microscopic images of cellular morphology. Methylmercury and thimerosal caused significant dose-dependent alterations in the morphology of Caco-2 cells relative to untreated control cells (Figure 5A and B, respectively). These data revealed that mercury, as both methylmercury and thimerosal, caused substantial morphological alterations in Caco-2 cells indicative of cytotoxicity.

NBMI protects against mercury-induced cell morphology alterations in colon epithelial cells

After observing that NBMI attenuated mercury-induced cytotoxicity in Caco-2 cells, we sought to investigate whether morphological alterations in Caco-2 cells would be attenuated by NBMI. To study this, Caco-2 cells were pre-treated with NBMI (50 μM) for 1 h prior to treatment with methylmercury (10 μM) and thimerosal (25 μM) for 1 h. Following treatment, we visually captured images of microscopic cellular morphology.

NBMI significantly attenuated mercury-induced morphological alterations in Caco-2 cells (Figure 6). These results revealed that NBMI is effective in attenuating cytotoxic alterations in cellular morphology caused by methylmercury and thimerosal.

Mercury inhibits proliferation of colon epithelial cells and NBMI protects against mercury-induced inhibition of proliferation of colon epithelial cells

In this study, we have shown that NBMI protects against mercury-induced cytotoxicity in Caco-2 cells. These results led us to investigate whether NBMI would also ameliorate mercury-induced inhibition of cellular proliferation. To examine this possibility, we measured [^{3}H]-thymidine incorporation after Caco-2 cells were pre-treated with NBMI (50 μM) for 1 h prior to treatment with methylmercury (10 μM) and thimerosal (25 μM) for 1 h. Significant decreases in [^{3}H]-thymidine incorporation were observed in Caco-2 cells treated with mercury, relative to untreated control cells. Furthermore, NBMI significantly attenuated methylmercury- and thimerosal-induced decreases in [^{3}H]-thymidine incorporation (Figure 7A and B, respectively). These data demonstrated that mercury inhibits cellular proliferation and NBMI ameliorates mercury-induced inhibition of cellular proliferation.

Mercury enhances ROS production in colon epithelial cells and NBMI attenuates mercury-induced ROS production in colon epithelial cells

Earlier, we reported that mercury causes cytotoxicity in BPAECs through generation of ROS. This finding and our early demonstration that mercury causes cytotoxicity in Caco-2 cells led us to investigate whether mercury causes cytotoxicity in

Caco-2 cells through generation of intracellular ROS. To investigate this possible mechanism, we measured the formation of intracellular ROS using DCFDA following treatment with methylmercury (10 μM) and thimerosal (25 μM) for 30 min. Caco-2 cells treated with mercury exhibited significant increases in DCFDA fluorescence relative to untreated control cells. Furthermore, NBMI significantly attenuated mercury-induced increases in DCFDA fluorescence to near control levels (Figure 8). Collectively, this data suggests that mercury-induced cytotoxicity in Caco-2 cells occurs through significant, temporally upstream generation of ROS and NBMI is effective in attenuating mercury-induced ROS generation.

Mercury depletes GSH (thiol-redox) in colon epithelial cells and NBMI stabilizes depletion of GSH in colon epithelial cells

Previous studies have shown that generation of intracellular ROS leads to a depletion of glutathione (GSH). This finding and our observation that mercury-induced cytotoxicity in Caco-2 cells occurs through significant generation of ROS led us to study whether depletion of GSH occurs concomitantly with mercury-induced cytotoxicity in Caco-2 cells. To investigate this possible mechanism, Caco-2 cells were pre-treated with NBMI (50 μM) for 1 h prior to treatment with methylmercury (10 μM) and thimerosal (25 μM) for 2 h. Following treatment, intracellular level of GSH were measured spectrophotometrically. Caco-2 cells treated with mercury exhibited significant decreases in GSH levels relative to untreated controls. In addition, NBMI stabilized mercury-induced depletion of GSH to near control levels (Figure 9). This data suggested that

mercury-induced generation of ROS led to GSH depletion and NBMI stabilized mercury-induced GSH diminution in Caco-2 cells.

Mercury causes loss of TEPCR (barrier dysfunction) in a dose- and time-dependent fashion

Oxidants were shown in earlier studies to induce changes in cell-to-cell adhesions that result in a drop in electrical resistance across epithelial and endothelial monolayers (Sliman et al., 2009 and Elton et al., 200X). To further investigate our hypothesis that mercury contributes to leaky gut syndrome through disrupting cell-to-cell adhesion within the colonic epithelium, Caco-2 cells were treated with methylmercury (1, 5, and 10 μM) and thimerosal (5, 10, and 25 μM) and changes in electrical resistance across confluent monolayers were measured in real time for 6 h via ECIS. Methylmercury (5 and 10 μM) produced significant time- and dose-dependent decreases in electrical resistance in comparison to untreated control cells (Figure 10A & B). Thimerosal (5, 10, and 25 μM) also exhibited significant time-and dose-dependent diminution of electrical resistance relative to untreated control cells (Figure 10C & D). These data showed, for the first time, that mercury caused significant time- and dose-dependent losses in cell-to-cell adhesion in Caco-2 cells.

NBMI attenuates mercury-induced barrier dysfunction

NBMI, which previously in this study demonstrated attenuation of mercury-induced cytotoxicity, generation of ROS, and depletion of intracellular thiols, was next evaluated for efficacy in preventing mercury-induced barrier dysfunction. Caco-2 cells

were treated with NBMI (50 μM) alone, thimerosal (25 μM) alone, or co-treated with NBMI (50 μM) and thimerosal (25 μM) together and electrical resistance was measured in real time for 6 h using ECIS. NBMI effectively attenuated thimerosal-induced decreases in electrical resistance across confluent monolayers to levels near untreated control cells (Figure 11). Consequently, this data demonstrated NBMI was effective in ameliorating mercury-induced barrier dysfunction in Caco-2 cells.

Mercury enhances paracellular transport of macromolecules (FITC-Dextran) across colon epithelial cell layers and NBMI attenuates paracellular leak in colon epithelial cell layers

Previously, we observed that mercury induces barrier dysfunction resulting in transcellular leak across the intestinal epithelium. We therefore sought to investigate whether mercury induces paracellular leak in Caco-2 cells. To determine paracellular transport of macromolecules across layers of Caco-2 cells, we used the FITC-Dextran permeability assay in which florescence is an indication of the leak that occurs across a membrane. Caco-2 cells were co-treated with NBMI (50 μM) and methylmercury (10 μM) or thimerosal (25 μM) for 2 h. Following treatment fluorescence was measured as an indication of leak. Caco-2 cells treated with mercury had significant increases in fluorescence relative to untreated controls. In addition, NBMI significantly attenuated mercury-induced increase in fluorescence (Figure 12). These results reveal that mercury enhances paracellular transport of macromolecules across Caco-2 cell layers and NBMI is effective in attenuating mercury-induced paracellular leak.

Mercury causes actin stress fiber formation which is attenuable through NBMI treatment

Cytoskeletal rearrangements in colonic epithelial cells, including the formation of actin stress fibers, have been repeatedly established with leaky gut syndrome. However, the formation of actin stress fibers in response to mercury in Caco-2 cells has never been investigated. Here, we hypothesized that mercury would cause formation of actin stress fibers resultant from ROS generation, which was previously demonstrated. To test our hypothesis, Caco-2 cells were treated with NBMI (50 μM) alone, mercury (methylmercury [10 μM] and thimerosal [25 μM]) alone, or co-treated with NBMI (50 μM) and mercury together for 30 min. Following treatment, cells were stained with actin-specific monoclonal antibodies and visualized with fluorescent confocal microscopic immunohistochemistry. Mercury caused significant dose-dependent increases in actin stress fiber formation which were attenuated by NBMI (Figure 13). This experiment substantiated the notion that mercury could potentially contribute to leaky gut syndrome through inducing cytoskeletal rearrangements in colonic epithelial cells.

NBMI attenuates mercury-induced alterations in intercellular adhesions

Having shown mercury causes paracellular leak and cytoskeletal rearrangements in Caco-2 cells, we next investigated whether mercury would affect cell-to-cell adhesion proteins. We evaluated this potential effect through the use of fluorescent confocal microscopic immunohistochemistry with ZO-1- and occludin-specific antibodies. Caco-2 cells were treated with NBMI (50 μM) alone, mercury (methylmercury [10 μM] and thimerosal [25 μM]) alone, or co-treated with NBMI (50 μM) and mercury together for

30 min and then stained, fixed, mounted, and images were captured digitally. Both thimerosal and methylmercury caused significant alterations in ZO-1 and occludin intracellular staining which were attenuated by NBMI (Figure 14). This data further substantiated the notion that mercury contributes to leaky gut syndrome through disrupting the integral membrane proteins which form tight junctions in the colonic epithelium.

DISCUSSION

The results of the current study revealed that the two forms of mercury, methylmercury (organic form) and thimerosal (pharmaceutical form) caused cytotoxicity, depletion of intracellular GSH, enhanced formation of ROS, decreased cell proliferation, barrier dysfunction, increased paracellular transport of macromolecules, actin cytoskeletal reorganization, and tight-junction alterations in the Caco-2 colon epithelial cells. Furthermore, the results of the current study also demonstrated that the novel thiol-redox-stabilizing antioxidant and heavy metal chelating drug, NBMI effectively attenuated the mercury-induced cytotoxicity, tight junction alterations, and increase in paracellular leak in Caco-2 cells. This is the first evidence which demonstrated that mercury induced intestinal epithelial cell damage, cytoskeletal and tight junction alterations, and macromolecule leak through thiol-redox depletion and oxidative stress which was effectively protected by the novel thiol-redox stabilizer, NBMI.

Mercury is a serious environmental pollutant, occupational hazard, and pharmaceutical toxicant (Hagele et al.). Mercury-containing dental amalgams have been identified to contribute mercury toxicity in humans (McCullough and Tyas 2008). Mercury, both inorganic and organic forms, has been established as potent toxic heavy metal with cytotoxic, neurotoxic, and teratogenic effects. Mercury-induced neuronal cell death and neurotoxicity have been reported (Choi et al. 2011). Mercury has also been shown to cause mitochondria-dependent apoptosis in hepatocytes (Pal et al. 2012). Inorganic mercury has been observed to cause pancreatic beta-cell death through oxidative stress-mediated apoptosis and necrosis (Chen et al. 2010). Trolox, a water-

soluble form of vitamin E, has been demonstrated to prevent methylmercury-induced ROS generation and neurotoxicity in glial cells (Kaur et al. 2010). In neurons, methylmercry has been shown to cause cytotoxicity through oxidative stress (Zhang et al. 2009). Cytotoxicity of thimerosal has been reported to be mediated by thiol-modulated mechanism (Wu et al. 2008). Role of ROS and thiol-redox depletion have been shown to mediate mercury-induced phospholipase A_2 and D activation in vascular endothelial cells (Hagele; Mazerik). The involvement of glutamate and ROS in methylmercury neurotoxicity has been emphasized (Aschner et al. 2007). It has also been shown that N-acetyl-L-cysteine (NAC) and the novel thiol-redox antioxidant and heavy metal chelating agent, NBMI protects against mercury- and oxidant-induced activation of phospholipase D, GSH depletion, ROS generation, and oxidative stress in vascular endothelial cells (Secor et al. 2011; Patel et al. 2012). These reports offer substantial support in favor of the findings of the current study that mercury (both methylmercury and thimerosal) caused ROS- and thiol-redox-mediated cytotoxicity in the Caco-2 colon epithelial cells that was protected by the thiol-redox stabilization by the classic thiol protectant, NAC and the novel lipophilic thiol-redox antioxidant and heavy metal chelator, NBMI.

Studies with *in vivo* mouse model have revealed the endothelial barrier dysfunction and enhanced paracellular permeability in lung following bleomycin exposure (Yin et al. 2012). Tight junction proteins have been shown to be crucial for cellular contacts including the epithelial and endothelial cells of the ECs (Utech et al. 2006; Van Itallie and Anderson, 2006). Zonula occludens-1 (ZO-1) and occludins are important tight junction proteins. The actin-cytoskeleton is important machinery for the maintenance of

the cellular architecture for proper physiological functions and the intestinal epithelial cells including the Caco-2 cells are no exception to this. The actin microfilaments have been recognized as the critical players in the regulation of endothelial barrier and similar regulation of the intestinal barrier by the epithelial cytoskeleton is expected (Dudek and Garcia, 2001). The ZO-1 and actin-cytoskeleton are tightly associated and if this association is altered, the barrier function and paracellular permeability are dysregulated as seen in the endothelial cell monolayers (Kawkitinarong et al. 2004). Oxidants and oxidative stress alter the architecture and function of the cytoskeletal and tight junction protein machinery and association through thiol-redox dysregulation, wherein the intracellular GSH dysregulation plays a major role. ROS and the lipid peroxidation-generated reactive carbonyl, 4-hydroxy-2-nonenal (4-HNE) have been recognized as potent disruptors of the cytoskeletal-tight junction assembly leading to the endothelial barrier dysfunction in the lung microvessels (Usatyuk et al. 2006; Uchida 2003). The hyperglycemic oxoaldehyde and the advanced glycation endproduct precursor, glyoxal, has been shown to cause endothelial barrier dysfunction that is associated with the actin cytoskeletal rearrangement and tight junction protein alterations (Sliman et al. 2010). Oxidants including hydrogen peroxide and diamide have been demonstrated to cause the disruption of the tight junction proteins such as ZO-1 and occludins leading to the altered epithelial barrier function (Chapman et al. 2002; Usatyuk et al. 2003). Mercury has been shown to cause neurocytotoxicity and cytoskeletal reorganization in chick embryo neurons (Choi et al. 2011). Thiol-protectants including NAC have been shown to protect against the oxidant-induced endothelial barrier disruption (Usatyuk et al. 2003). In Caco-2 cells, it has been shown that mercury causes tight junction alterations with altered beta-

actin synthesis and paracellular permeability (Calabro et al. 2011). This study signifies that mercury disrupts intestinal barrier function through tight junction alterations. In addition, another study reveals that methylmercury causes cytotoxicity in Caco-2 cells as demonstrated by the capillary zone electrophoresis (Zhang et al. 2012). Therefore, the results of the current study concurred with these findings demonstrating that the mercury-induced cytoskeletal reorganization, tight junction protein alterations, and barrier dysfunction in the Caco-2 colon epithelial cells were caused by mercury through oxidative stress and thiol-redox alterations. In addition, this study clearly revealed that the novel thiol-redox antioxidant and heavy metal chelator, NBMI was an effective agent in protecting against the mercury-induced actin cytoskeletal rearrangement, tight junction protein alterations, and enhanced paracellular permeability of macromolecules in the Caco-2 colon epithelial cells in culture, apparently through the stabilization of intracellular thiol-redox, scavenging/quenching of ROS, and chelating the toxic mercury species.

On the whole, the results of the current study clearly demonstrated that both forms of mercury (methylmercury and thimerosal) caused cytotoxicity, generation of ROS, loss of thiols, increase in paracellular permeability, cytoskeletal reorganization, tight junction protein alterations, and barrier dysfunction in the Caco-2 colon epithelial cells and these adverse cellular effects were all protected by the thiol-protectants suggesting the role of thiol-redox dysregulation in the mercury-induced epithelial cytotoxicity and barrier dysfunction (Schema-1). Besides, this study was the first observation to demonstrate that the novel lipid-soluble thiol-protectant, NBMI, was more effective as compared to the

commonly used water-soluble thiol-protectant (antioxidant), NAC, in offering protection against the mercury-induced cytotoxicity, oxidative stress, thiol-redox dysregulation, cytoskeletal rearrangement, tight junction protein alterations, and barrier dysfunction in the colon epithelial cells. Above all, the current study also demonstrated that NBMI offered effective protection against the mercury-induced toxicity at μM dose, whereas mM concentration of NAC was required to achieve such protection in the Caco-2 colon epithelial cells. Structurally, NBMI resembles the dicarboxybenzoate moiety bound to two cysteamines as found naturally in fruits. Therefore, NBMI is expected to act as both heavy metal chelator and free radical scavenger. The ability of NBMI to complex with trace heavy metals has been reported (Zaman et al. 2007). Thus, mercury could have been also chelated by NBMI in addition to the ability of NBMI acting as an antioxidant and thiol-protecting agent against the mercury-induced oxidative stress as observed in the current study in the Caco-2 colon epithelial cells. Furthermore, the lipophilic nature of NBMI could have offered advantage to the molecule to selectively partition in the lipid-rich hydrophobic microenvironments of the cellular membranes where the redox-regulated cellular reactions take place and thus protecting against the mercury-induced toxicity in the colon epithelial cells. The novel bifunctional chelating drug, such as NBMI, with thiol-redox stabilizing and antioxidant actions and heavy metal chelating ability appears as a promising therapeutic agent against the mercury- and oxidant-induced intestinal epithelial damage.

The rationale for the current work hinges on the leaky intestine, leaky-gut syndrome, and pediatric intestinal diseases (Liu et al. 2005). Tight junctions have been identified as

crucial players in regulating the barrier for paracellular transport in the intestine and disruption of the tight junctions has been connected with the conditions of intestinal hyperpermeability such as the leaky-gut syndrome (Liu et al. 2005). Oxidative and nitrosative stress have been recognized as important players in leaky-gut syndrome and the associated cardiovascular disorders (Maes and Twisk, 2009). Mercury has been implicated in cardiovascular diseases, autism, and neurological disorders (Hagele et al.). Therefore, the role of mercury in the etiology of leaky-gut syndrome may be emphasized. Along these lines, the protective role of thiol-redox stabilizers, especially the novel thiol-redox antioxidant and heavy metal chelator, NBMI against mercury-induced cytotoxicity and paracellular hyperpermeability in the intestinal epithelium appears to offer pharmacological intervention of leaky-gut syndrome, wherein ROS, thiol-redox dysregulation, and oxidative stress play a critical mechanistic role.

REFERENCES

1. Aschner M, Syversen T, Souza DO, Rocha JBT, and Farina M. Involvement of glutamate and reactive oxygen species in methylmercury neurotoxicity. *Brazilian Journal of Medical and Biological Research*, 2007; 40: 285-291.
2. Calabro AR, Gazarian DI, Barile FA. Effect of metals on beta-actin and total protein synthesis in cultured human intestinal epithelial cells. *J Pharmacol Toxicol Methods*, 2011, 63:47-58.
3. Chapman KE, Waters CM, Miller WM. 2002. Continuous exposure of airway epithelial cells to hydrogen peroxide: protection by KGF. *J Cell Physiol* 192:71–80.
4. Chen YW, Huang CF, Yang CY, Yen CC, Tsai KS, Liu SH. Inorganic mercury causes pancreatic beta-cell death via oxidative stress-induced apoptotic and necrotic pathways. *Toxicol Appl Pharmacol*, 2010, 243:323-31.
5. Choi WS, Kim SJ, Kim JS. Inorganic lead (Pb)- and mercury-induced neuronal cell death involves cytoskeletal reorganization. *Lab Animal Res*, 2011, 27:219-25.
6. Clarke D, Buchanan R, Gupta N, and Haley B. Amelioration of Acute Mercury Toxicity by a Novel, Non-Toxic Lipid Soluble Chelator N,N′bis-(2-mercaptoethyl)isophthalamide: Effect on Animal Survival, Health, Mercury Excretion and Organ Accumulation. *Toxicol Environ Chem*, 2012; 94(3): 616–640.
7. Dopp E, von Reckinghausen U, Hippler J, Diaz-Bone RA, Richard J, Zimmermann U, Rettenmeier AW, and Hirner AV. Toxicity of Volatile

Methylated Species of Bismuth, Arsenic, Tin, and Mercury in Mammalian Cells In Vitro. *Journal of Toxicology*, 2011: 1-7.

8. Dudek SM, Garcia JG. 2001. Cytoskeletal regulation of pulmonary vascular permeability. *J Appl Physiol* 91:1487–1500.

9. Fasano A and Shea-Donohue T. Mechanisms of Disease: the role of intestinal

10. Fasano A. Zonulin and Its Regulation of Intestinal Barrier Function: The Biological Door to Inflammation, Autoimmunity, and Cancer. *Physiol Rev*, 2011; 91: 151-175.

11. Francoa JL, Possera T, Missauc F, Pizzolattic MG, dos Santos A, Souzaf DO, Aschnerg M, Rochad JBT, Dafrea AL, and Farina M. Structure-activity relationship of flavonoids derived from medicinal plants in preventing methylmercury-induced mitochondrial dysfunction. *Environ Toxicol Pharmacol*, 2010; 30(3): 272–278.

12. Garrecht M and Austin DW. The plausibility of a role for mercury in the etiology

13. Groschwitz KR and Hogan SP. Intestinal barrier function: Molecular regulation and disease pathogenesis. *J Allergy Clin Immunol*. 2009;124:3-20.

14. Hagele TJ, Mazerik JN, Gregory A, Kaufman B, Magalang U, Kuppusamy ML, Marsh CB, Kuppusamy P, Parinandi NL. Mercury activates vascular endothelial cell phospholipase D through thiols and oxidative stress. *Int J Toxicol.* 2007 Jan-Feb;26(1):57-69.

15. Kaur P, Evje L, Aschner M, Syversen T. The in vitro effects of Trolox on methylmercury-induced neurotoxicity. *Toxicology*, 2010, 30:73-8.

16. Kawkitinarong K, Linz-McGillem L, Birukov KG, Garcia JG. 2004. Differential regulation of human lung epithelial and endothelial barrier function by thrombin. *Am J Respir Cell Mol Biol* 31:517–527.

17. Liu Z, Li N, Neu J. Tight junctions, leaky intestines, and pediatric diseases. Acta Paediatr. 2005; 94:386-93.

18. Ma TY, Tran D, Hoa N, Donnguyen, Merryfield M, and Tarnawski A. Mechanism of Extracellular Calcium Regulation of Intestinal Epithelial Tight Junction Permeability: Role of Cytoskeletal Involvement. *Microsc. Res. Tech,* 2000; 51:156–168.

19. Maes M, Twisk FN. Why myalgic encephalomyelitis/chronic fatigue syndrome (ME/CFS) may kill you: disorders in the inflammatory and oxidative stress (IO&NS) pathways may explain cardiovascular disorders in ME/CFS. *Neuro Endocrinol Lett*, 2009; 677-93.

20. Magistris L, Familiari V, Pascotto A, Sapone A, Frolli A, Iardino P, Carteni M, De Rosa M, Francavilla R, Riegler G, Militerni R, and Bravaccio C. Alterations of the Intestinal Barrier in Patients With Autism Spectrum Disorders and in Their First-degree Relatives. *JPGN*, 2010; 51:418-424.

21. Makani S, Gollapudi S, Yel L, Chiplunkar S, and Gupta S. Biochemical and molecular basis of thimerosal-induced apoptosis in T cells: a major role of mitochondrial pathway. *Genes and Immunity*, 2002; 3: 270–278.

22. Mazerik JN, Hagele T, Sherwani S, Ciapala V, Butler S, Kuppusamy ML, Hunter M, Kuppusamy P, Marsh CB, Parinandi NL. Phospholipase A2 activation

regulates cytotoxicity of methylmercury in vascular endothelial cells. *Int J Toxicol.* 2007 Nov-Dec;26(6):553-69.

23. McCullough MJ, Tyas MJ. Local adverse effects of amalgam restorations. *Int Dent J*, 2008, 58:3-9.
24. Patel PB, Pal S, Das J, Sil PC. Modulation of mercury-induced mitochondria-dependent apoptosis by glycine in hepatocytes. *Amino Acids*, 2012, 42:1669-83.
25. Patel RB, Kotha SR, Sauers LA, Malireddy S, Gurney TO, Gupta NN, Elton TS, Magalang UJ, Marsh CB, Haley BE, Parinandi NL. Thiol-redox antioxidants protect lung vascular endothelial cytoskeletal alterations caused by pulmonary fibrosis inducer, bleomycin: comparison between classical thiol-protectant, N-acetyl-L-cysteine, and novel thiol antioxidant, N,N'-bis-2-mercaptoethyl isophthalamide. *Toxicol Mech Methods*, 2012, Feb. 1-14.
26. Secor JD, Kotha SR, Gurney TO, Patel RB, Kefauver NR, Gupta N, Morris AJ, Haley BE, Parinandi NL. Novel lipid-soluble thiol-redox antioxidant and heavy metal chelator, N,N'-bis(2-mercaptoethyl)isophthalamide (NBMI) and phospholipase D-specific inhibitor, 5-fluoro-2-indolyl des-chlorohalopemide (FIPI) attenuate mercury-induced lipid signaling leading to protection against cytotoxicity in aortic endothelial cells. In*t J Toxicol.* 2011, 30:619-38.
27. Shen L and Turner JR. Role of Epithelial Cells in Initiation and Propagation of Intestinal Inflammation. Eliminating the static: tight junction dynamics exposed. *Am J Physiol Gastrointest Liver Physiol*,2006; 290:G577-G582.
28. Sliman SM, Eubank TD, Kotha SR, Kuppusamy ML, Sherwani SI, Butler ES, Kuppusamy P, Roy S, Marsh CB, Stern DM, Parinandi NL. Hyperglycemic

oxoaldehyde, glyoxal, causes barrier dysfunction, cytoskeletal alterations, and inhibition of angiogenesis in vascular endothelial cells: aminoguanidine protection. *Mol Cell Biochem.*2010 Jan;333(1-2):9-26.

29. Uchida K. 2003. 4-Hydroxy-2-nonenal: a product and mediator of oxidative stress. *Prog Lipid Res* 42:318–343.

30. Usatyuk PV, Vepa S, Watkins T, He D, Parinandi NL, Natarajan V. 2003. Redox regulation of reactive oxygen species-induced p38 MAP kinase activation and barrier dysfunction in lung microvascular endothelial cells. *Antioxid Redox Signal* 5:723–730.

31. Usatyuk PV, Parinandi NL, Natarajan V. 2006. Redox regulation of 4-hydroxy-2-nonenalmediated endothelial barrier dysfunction by focal adhesion, adherens, and tight junction proteins. *J Biol Chem* 281:35554–35566.

32. Utech M, Brüwer M, Nusrat A. 2006. Tight junctions and cell-cell interactions. *Methods Mol Biol* 341:185–195.

33. Van Itallie CM, Anderson JM. 2006. Claudins and epithelial paracellular transport. *Annu Rev Physiol* 68:403–429.

34. Wu X, Liang H, O'Hara KA, Yalowich JC, Hasinoff BB. Thiol-modulated mechanisms of the cytotoxicity of thimerosal and inhibition of DNA topoisomerase II alpha. *Chem Res Toxicol*, 2008, 21:483-93.

35. Yin Q, Nan H, Yan L, Huang X, Wang W, Cui G, Wei J. 2012. Alteration of tight junctions in pulmonary microvascular endothelial cells in bleomycin-treated rats. *Exp Toxicol Pathol* 64:81–91.

36. Zhang L, Qu F, Hu M, Ding J, Lou B. Capillary zone electrophoresis-based cytotoxicity analysis of Caco-2 cells. *Electrophoresis*, 2012, 33:834-40.
37. Zhang P, Xu Y, Sun J, Li X, Wang L, Jin L. Protection of pyrroloquinoline quinine against methylmercury-induced neurotoxicity via reducing oxidative stress. *Free Radic Res*, 2009, 43:224-33.

FIGURE LEGENDS

Figure 1. Chemical structures of mercuric compounds and antioxidants. (A) methylmercury chloride ($MeHgCl_2$) (B) Thimerosal (C) N-acetylcysteine (NAC) (D) dimercaptosuccinic acid (DMSA) (E) N-bis-mercaptoethylisopthalamide (NBMI)

Figure 2. Mercury induces cytotoxicity in colon epithelial cells. Caco-2 cells ($2.5x10^5$ cells/17.5-mm dish) were treated with MEM alone or MEM containing different concentrations (1, 5, 10 μM) of methylmercury or different concentrations (5, 10, 25 μM) of thimerosal for 1 and 2 hours. At the end of the incubation period, release of LDH into the medium (A&B) and decrease in MTT reduction (B&C) were determined spectrophotometrically. Data represent mean ± S.D. calculated from the independent experiments. *Significantly different at $P<0.05$ as compared to cells treated with MEM alone.

Figure 3. NBMI attenuates mercury-induced cytotoxicity in colon epithelial cells. Caco-2 cells ($2.5x10^5$ cells/17.5-mm dish) were pretreated with MEM alone or MEM containing different concentrations (10, 25, 50 μM) of NBMI for 1 hour. Pre-treated cells were then treated with MEM alone, MEM containing methylmercury (10 μM) or thimerosal (25 μM), or MEM containing methylmercury (10 μM) and NBMI (50 μM) or thimerosal (25 μM) and NBMI (50 μM) for 1 hour. At the end of the incubation period, release of LDH into the medium (A&B) and decrease in MTT reduction (B&C) were determined spectrophotometrically. Data represent mean ± S.D. calculated from the independent experiments. *Significantly different at $P<0.05$ as compared to cells treated with MEM alone. **Significantly different at $P<0.05$ as compared to cells treated with MEM containing methylmercury or thimerosal alone.

Figure 4. Comparison of NAC and DMSA with NBMI in attenuating mercury-induced cytotoxicity in colon epithelial cells. Caco-2 cells ($2.5x10^5$ cells/17.5-mm dish) were pretreated with MEM alone, MEM containing NBMI (50 μM), MEM containing NAC (50 μM) or MEM containing DMSA (50 μM) for 1 hour. Pre-treated cells were then treated with MEM alone, MEM containing methylmercury (10 μM; A) or thimerosal (25μM; B), or MEM containing methylmercury (10 μM) and NBMI (50 μM), NAC (50 μM), or DMSA (50 μM) or thimerosal (25 μM) and NBMI (50 μM), NAC (50 μM), or DMSA (50 μM) for 2 hours. At the end of the incubation period, release of LDH into the medium was determined spectrophotometrically. Data represent mean ± S.D. calculated from the independent experiments. *Significantly different at $P<0.05$ as compared to cells treated with MEM alone. **Significantly different at $P<0.05$ as compared to cells treated with MEM containing methylmercury or thimerosal alone.

Figure 5. Mercury causes alterations in cell morphology of colon epithelial cells. Caco-2 cells ($5x10^5$cells/25-mm dish) were treated with MEM alone, MEM containing different concentrations (1, 5, 10 μM) of methylmercury (A), or MEM containing different concentrations (5, 10, 25 μM) of thimerosal (B) for 1 hour. At the end of the incubation period, the cell morphology was examined under light microscope (as an index of cytotoxicity). Each micrograph is a representative picture obtained from 3 independent experiments conducted under identical conditions.

Figure 6. NBMI protects against mercury-induced cell morphology alterations in colon epithelial cells. Caco-2 cells ($5x10^5$cells/35-mm dish) were treated with MEM alone, MEM containing methylmercury (10 μM) or thimerosal (25 μM), or MEM containing methylmercury (10 μM) and NBMI (50 μM) or thimerosal (25 μM) and NBMI (50 μM)

for 1 hour. At the end of the incubation period, the cell morphology was examined under light microscope (as an index of cytotoxicity). Each micrograph is a representative picture obtained from 3 independent experiments conducted under identical conditions.

Figure 7. Mercury inhibits proliferation of colon epithelial cells and NBMI protection. Caco-2 cells ($5x10^5$cells/35-mm dish) were pretreated with MEM alone or MEM containing NBMI (50 μM) for 1 hour. Pre-treated cells were then treated with MEM alone, MEM containing methylmercury (10 μM) or thimerosal (25 μM), or MEM containing methylmercury (10 μM) and NBMI (50 μM) or thimerosal (25 μM) and NBMI (50 μM) for 1 hour. At the end of incubation, cells were labeled with [^{3}H]-thymidine (1 mCi/ml) in complete EC medium for 24 h. Cell replication at the end of the treatment was assayed by determining [^{3}H]-thymidine incorporated into the cells as described in *materials and methods*. Data represent means $\pm$ SD of independent experiment. * Significantly different at $P < 0.05$ as compared with the cells treated with MEM alone. **Significantly different at $P<0.05$ as compared to cells treated with MEM containing methylmercury or thimerosal alone.

Figure 8. Mercury enhances ROS production in colon epithelial cells and NBMI attenuation. Caco-2 cells ($5x10^5$cells/35-mm dish) were preloaded with 10 mmol/L DCFDA for 30 minutes in complete MEM to determine ROS generation. Following the DCDA loading, cells were subjected to treatment with MEM alone, MEM containing methylmercury (10 μM) or thimerosal (25 μM), or MEM containing methylmercury (10 μM) and NBMI (50 μM) or thimerosal (25 μM) and NBMI (50 μM) for 30 minutes. At the end of the incubation period, the DCFDA fluorescence (as an index of ROS formation) was determined as described under Materials and Methods section. Each

micrograph is a representative picture obtained from 3 independent experiments conducted under identical conditions. *Significantly different at P<0.05 as compared to cells treated with MEM alone. **Significantly different at *P*<0.05 as compared to cells treated with MEM containing methylmercury or thimerosal alone. DCFDA indicates 2'-7'-dichlorofluorescin diacetate; MEM, minimal essential medium; ROS, reactive oxygen species.

Figure 9. Mercury depletes GSH (thiol-redox) in colon epithelial cells and stabilization by NBMI. Caco-2 cells ($5x10^5$cells/96 well plates) were pretreated with MEM alone or MEM containing NBMI (50 μM) for 1 hour. Pre-treated cells were then treated with MEM alone, MEM containing methylmercury (10 μM) or thimerosal (25 μM), or MEM containing methylmercury (10 μM) and NBMI (50 μM) or thimerosal (25 μM) and NBMI (50 μM) for 2 hours to determine intracellular GSH levels. At the end of the incubation period, the intracellular soluble thiol (GSH) concentrations were determined. Data represent mean + SD calculated from 3 independent experiments. *Significantly different at P<0.05 as compared to cells treated with MEM alone. **Significantly different at *P*<0.05 as compared to cells treated with MEM containing methylmercury or thimerosal alone. GSH indicates glutathione.

Figure 10. Mercury causes loss of TEPCR (barrier dysfunction) in a dose- and time-dependent fashion. Caco-2 cell layers were cultured in complete MEM on gold electrodes and exposed to MEM alone or MEM containing different concentrations (1, 5, 10 μM; A&B) of methylmercury or different concentrations (5, 10, 25 μM; C&D) of thimerosal for 20 h in a humidified atmosphere of 5%CO_2-95% air at 37^{o}C and the TEPCR was measured continuously in an ECIS system as described in *materials and methods*. A and

C are representative tracings of the normalized resistance values of two independent experiments conducted under identical conditions. B and D is the graphical representation of the averaged normalized resistance values obtained from two independent determinations at specified time points. Data represent means $\pm$ SD of independent experiment.

Figure 11. NBMI attenuates mercury-induced loss of TEPCR (barrier dysfunction). Caco-2 cell layers were cultured in complete MEM on gold electrodes and exposed to MEM alone, MEM containing methylmercury (10 μM, A&C) or thimerosal (25 μM, B&D), or MEM containing methylmercury (10 μM) and NBMI (50 μM) or thimerosal (25 μM) and NBMI (50 μM) for 20 h in a humidified atmosphere of 5%CO_2-95% air at 37^{o}C and the TEPCR was measured continuously in an ECIS system as described in *materials and methods*. A and C are representative tracings of the normalized resistance values of two independent experiments conducted under identical conditions. B and D is the graphical representation of the averaged normalized resistance values obtained from two independent determinations at specified time points. Data represent means $\pm$ SD of independent experiment.

Figure 12. Mercury enhances paracellular transport of macromolecules (FITC-Dextran) across colon epithelial cell layers and NBMI attenuation. Caco-2 cells ($2.5x10^5$ cells/17.5-mm dish) were treated with MEM alone, MEM containing methylmercury (10 μM) or thimerosal (25 μM), or MEM containing methylmercury (10 μM) and NBMI (50 μM) or thimerosal (25 μM) and NBMI (50 μM) for 2 hours. At the end of incubation, FITC fluorescence (as an index of EC leak) was determined spectrophotometrically as described in *materials and methods*. Data represent means $\pm$ SD of independent

experiment. * Significantly different at $P < 0.05$ as compared with the cells treated with MEM alone. **Significantly different at $P<0.05$ as compared to cells treated with MEM containing methylmercury or thimerosal alone.

Figure 13. Mercury causes actin cytoskeleton rearrangements in colon epithelial cells and NBMI protection. Caco-2 cells ($5x10^5$cells/35-mm dish) were treated with MEM alone, MEM containing methylmercury (10 μM) or thimerosal (25 μM), or MEM containing methylmercury (10 μM) and NBMI (50 μM) or thimerosal (25 μM) and NBMI (50 μM) for 30 minutes. At the end of incubation, cells were fixed and stained for Actin Stress Fibers. Each image is a representative picture obtained from the independent experiment conducted under identical conditions.

Figure 14. Mercury induced tight junction alterations (ZO-1 and Occludins) in colon epithelial cells and NBMI protection. Caco-2 cells ($5x10^5$cells/35-mm dish) were treated with MEM alone, MEM containing methylmercury (10 μM) or thimerosal (25 μM), or MEM containing methylmercury (10 μM) and NBMI (50 μM) or thimerosal (25 μM) and NBMI (50 μM) for 30 minutes. At the end of incubation, cells were fixed and stained for Tight Junction Protein (ZO1) and Tight Junction Protein (Occludin) as described in materials and methods. Each image is a representative picture obtained from the independent experiment conducted under identical conditions.

Schema 1: Proposed mechanism of mercury-induced cytotoxicity in Caco-2 colon epithelial cells through ROS generation, thiol-redox dysregulation, inhibition of cell proliferation, mitochondrial dysfunction, tight junction alterations, cytoskeletal reorganization, and paracellular hyperpermeability.

Fig.1A

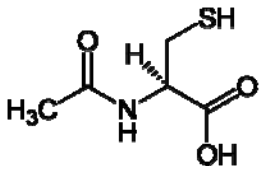

NAC

Fig.1B

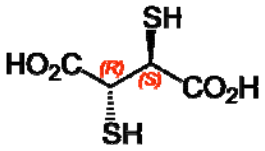

DMSA

Fig.1C

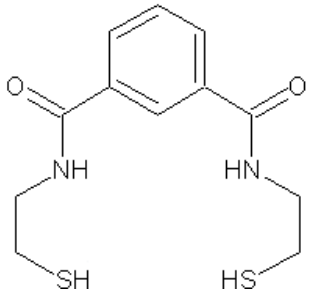

NBMI

Figure 2A

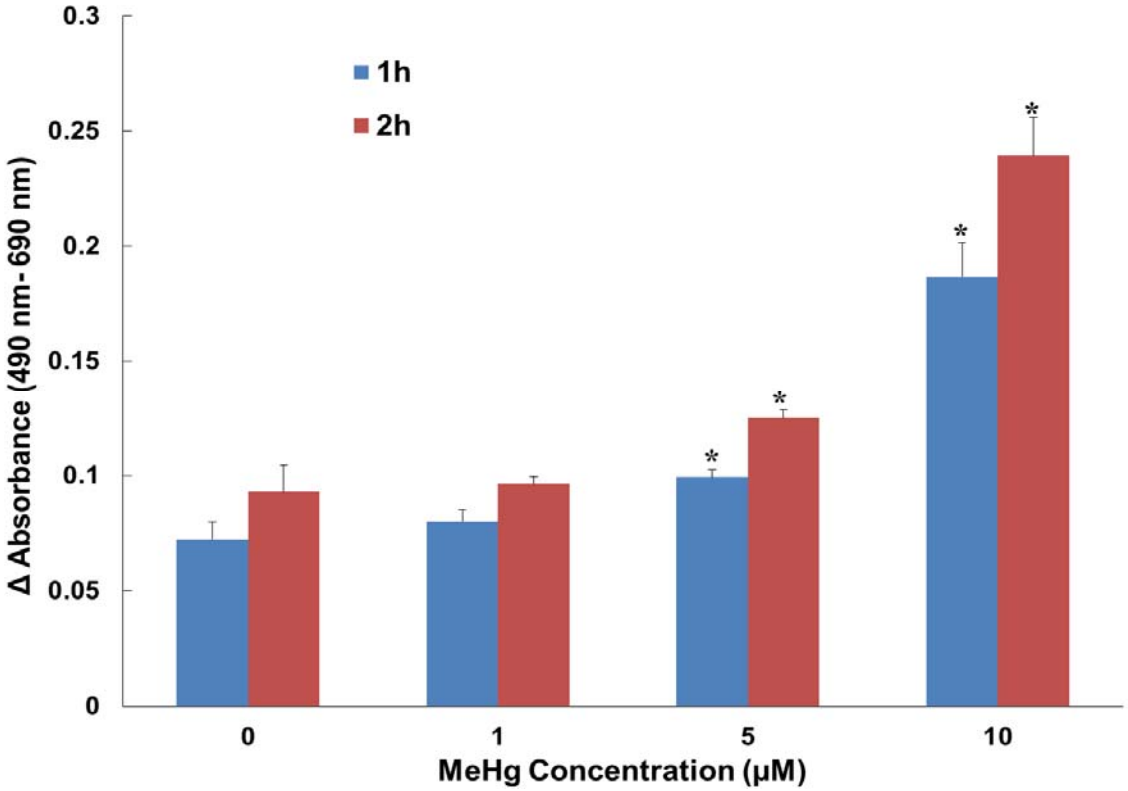

Figure 2B

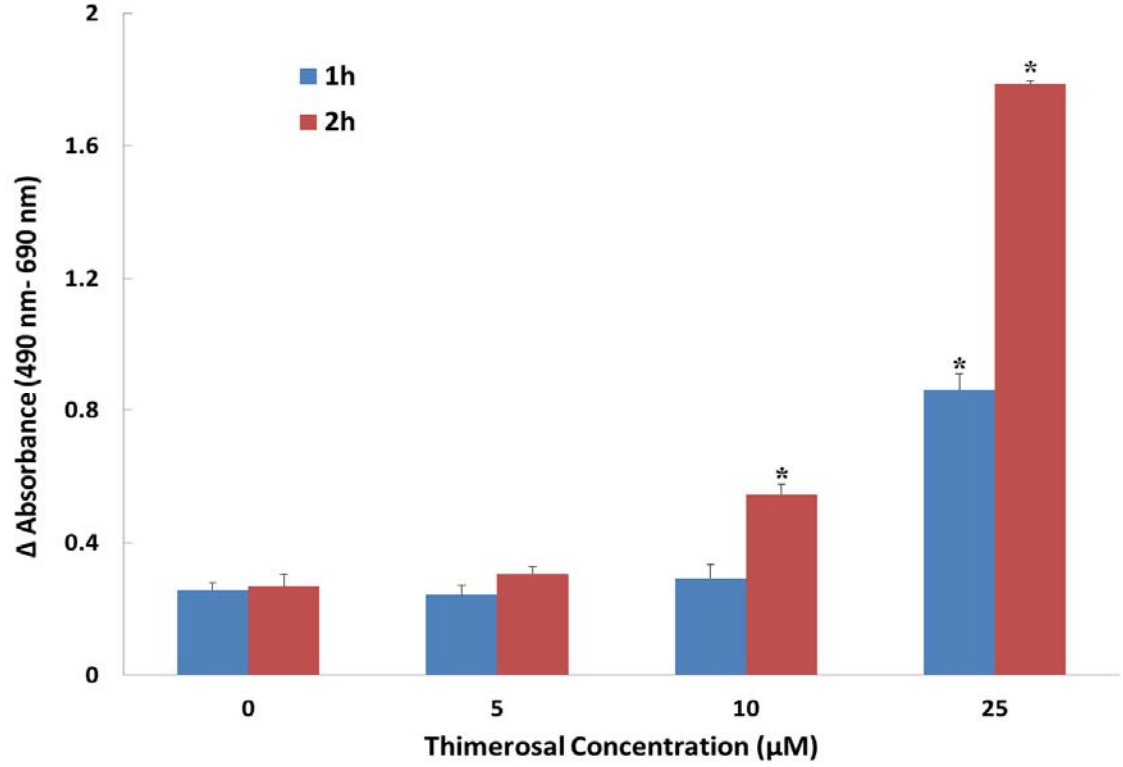

Figure 2C

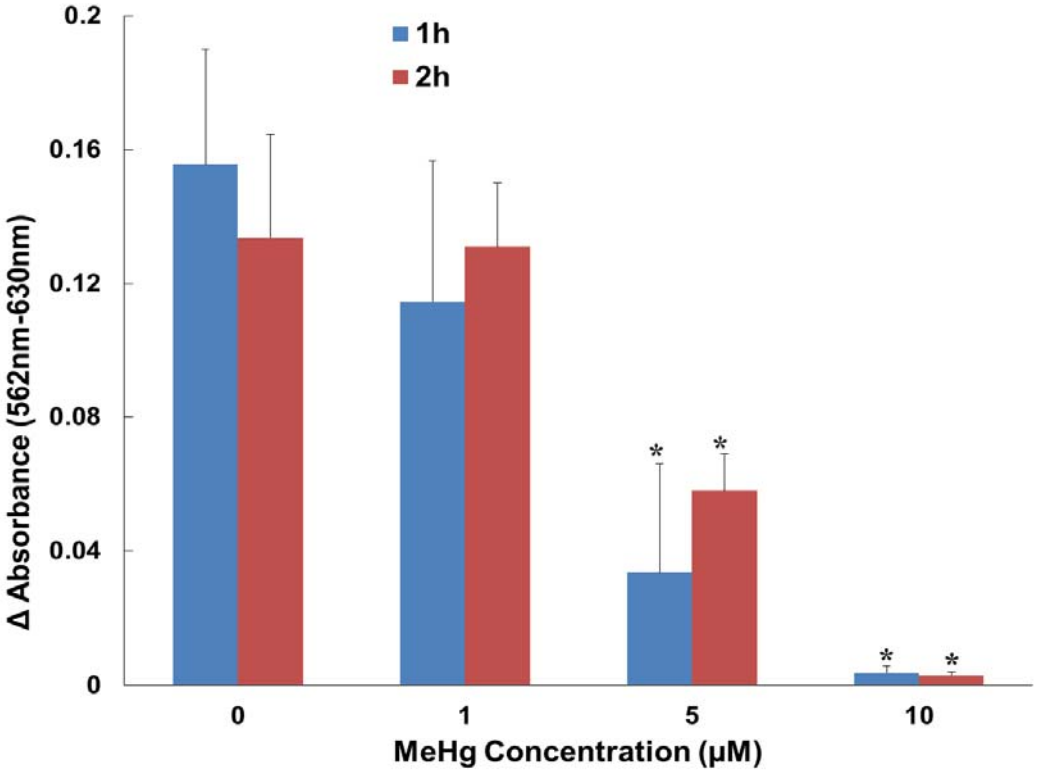

Figure 2D

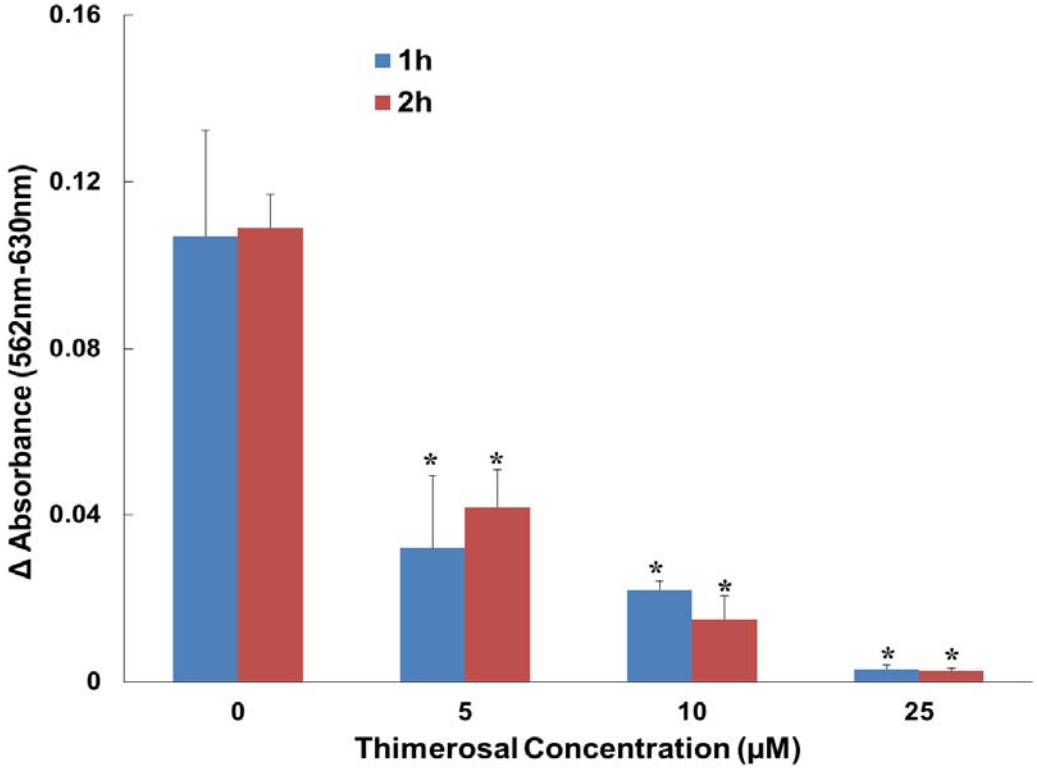

Figure 3A

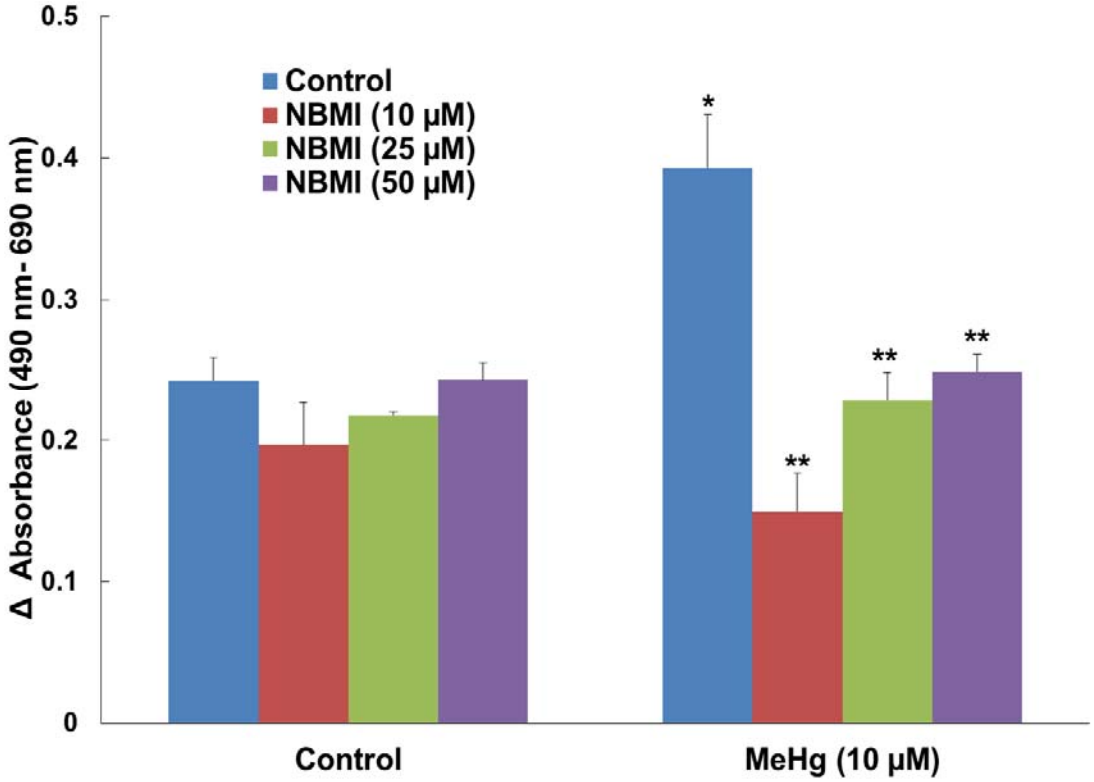

Figure 3B

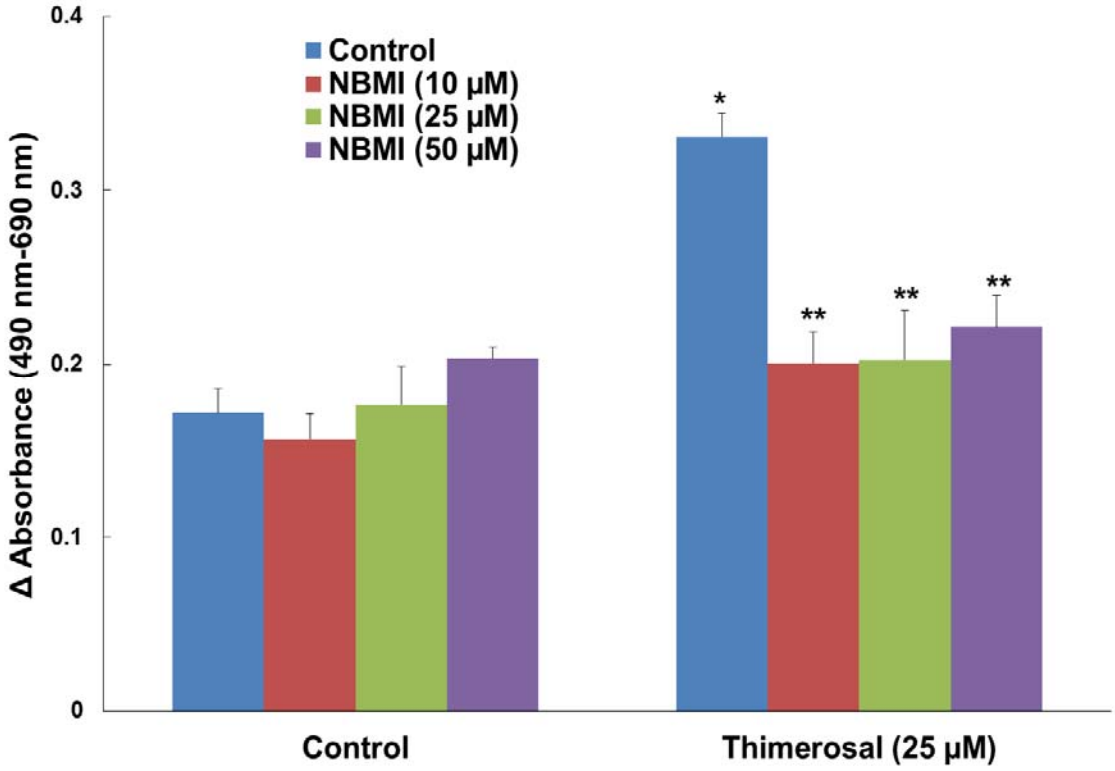

Figure 3C

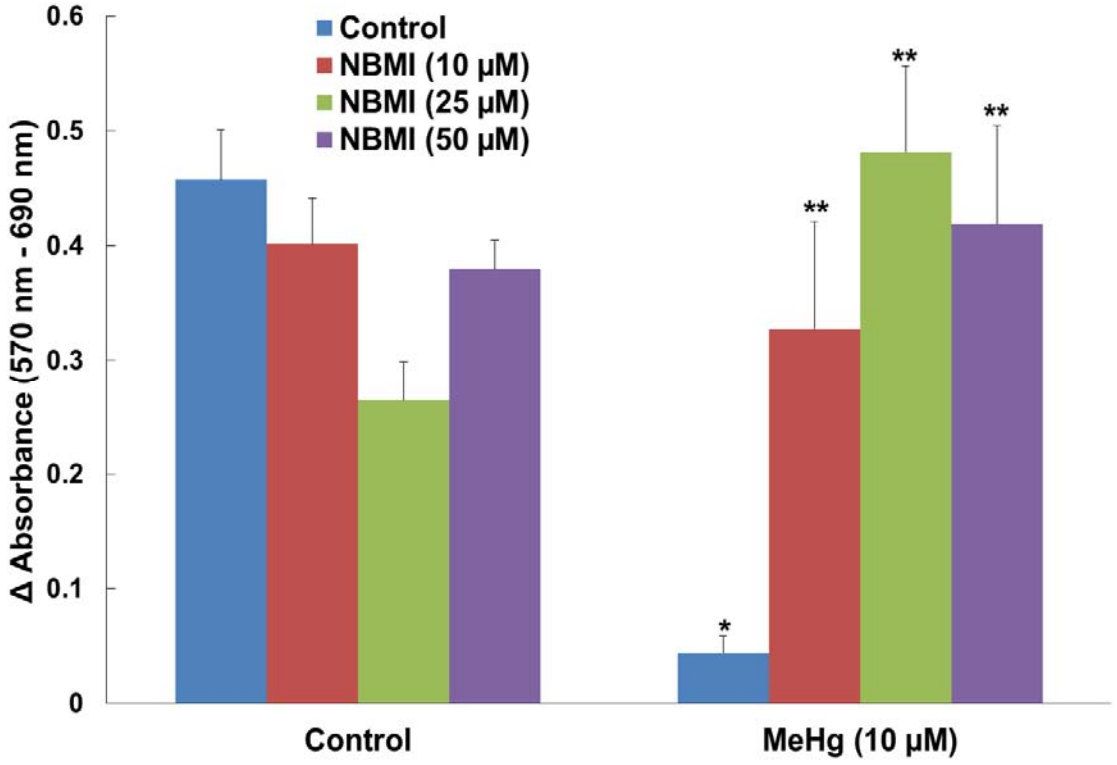

Figure 3D

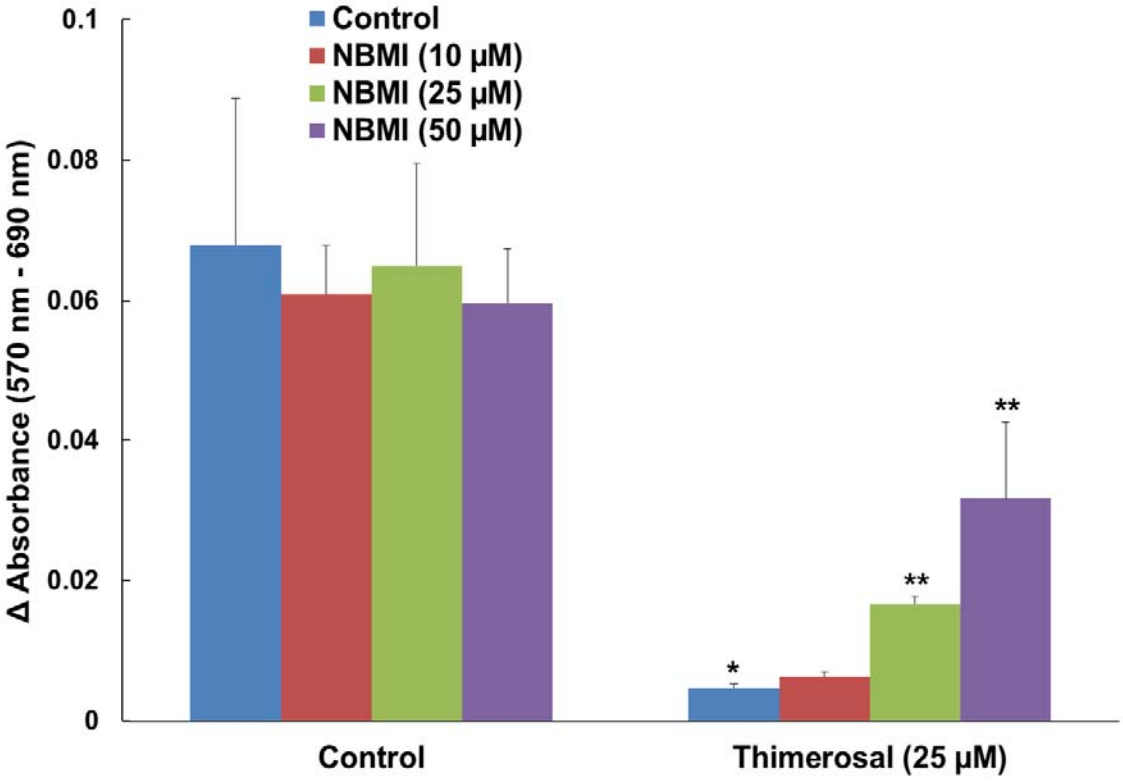

Figure 4A

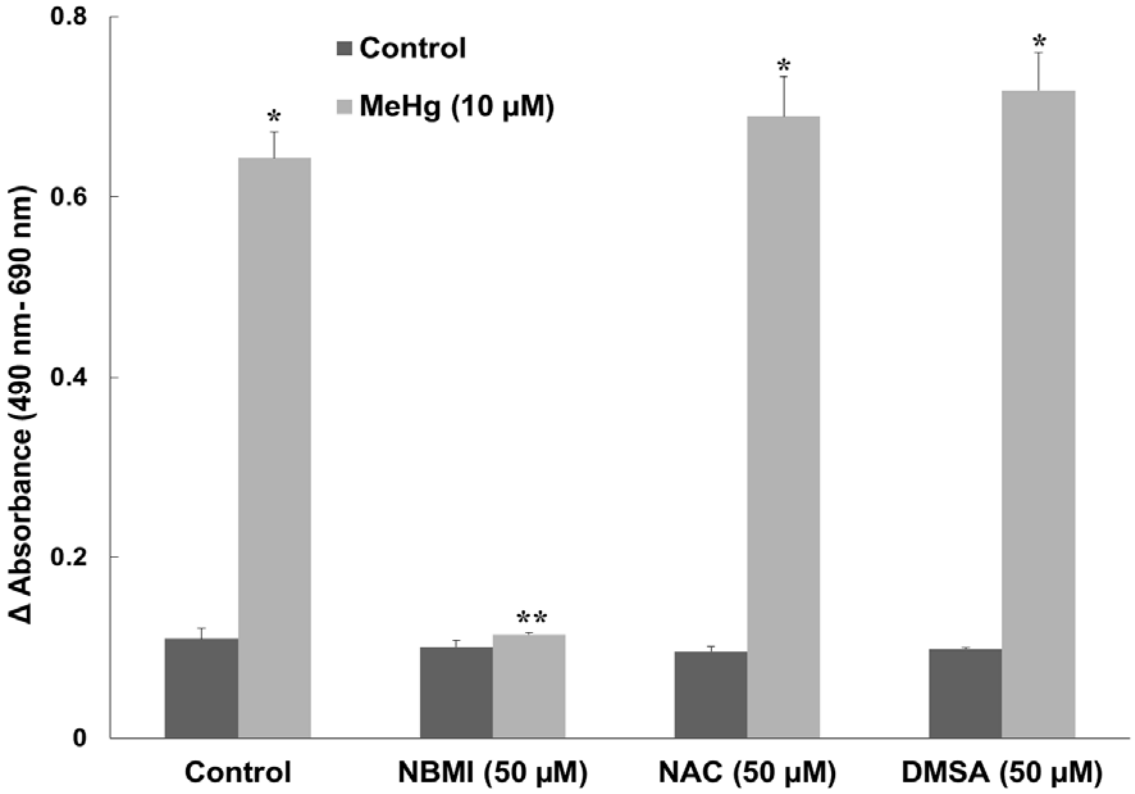

Figure 4B

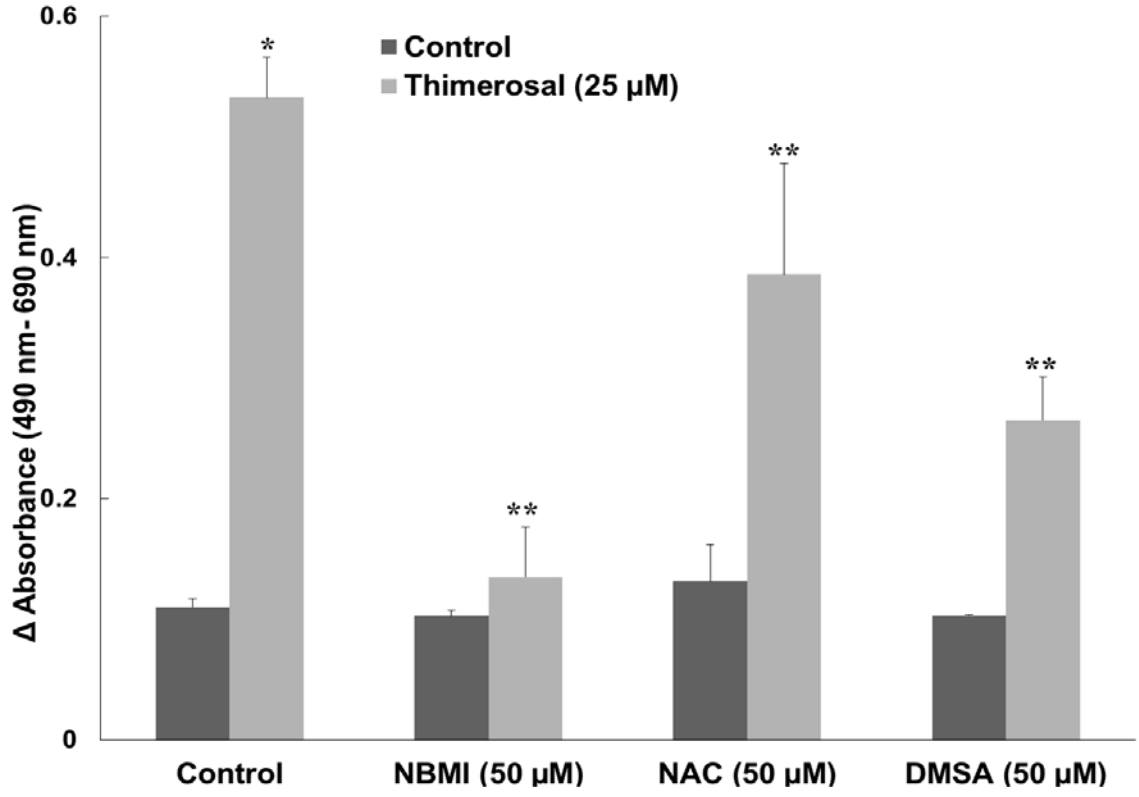

Figure 5A

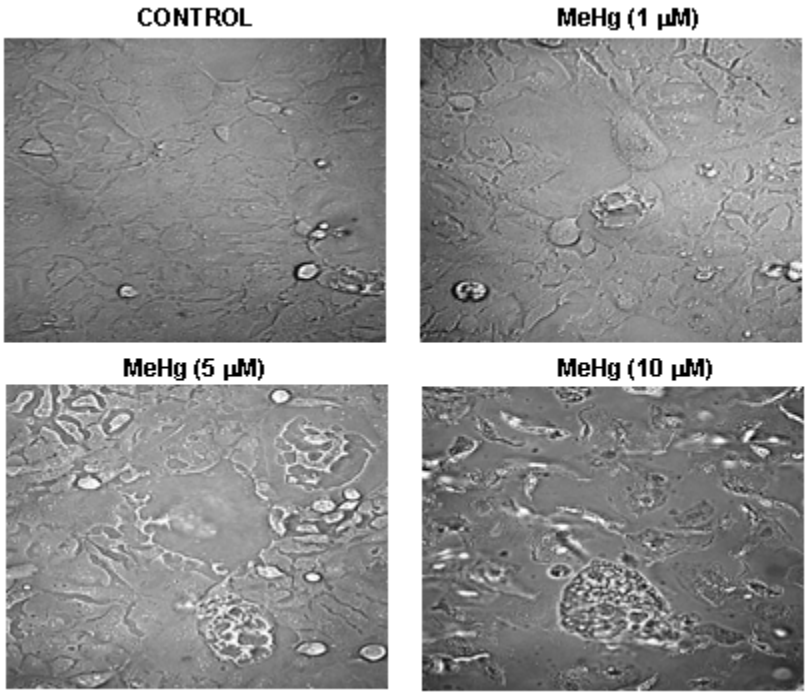

Figure 5B

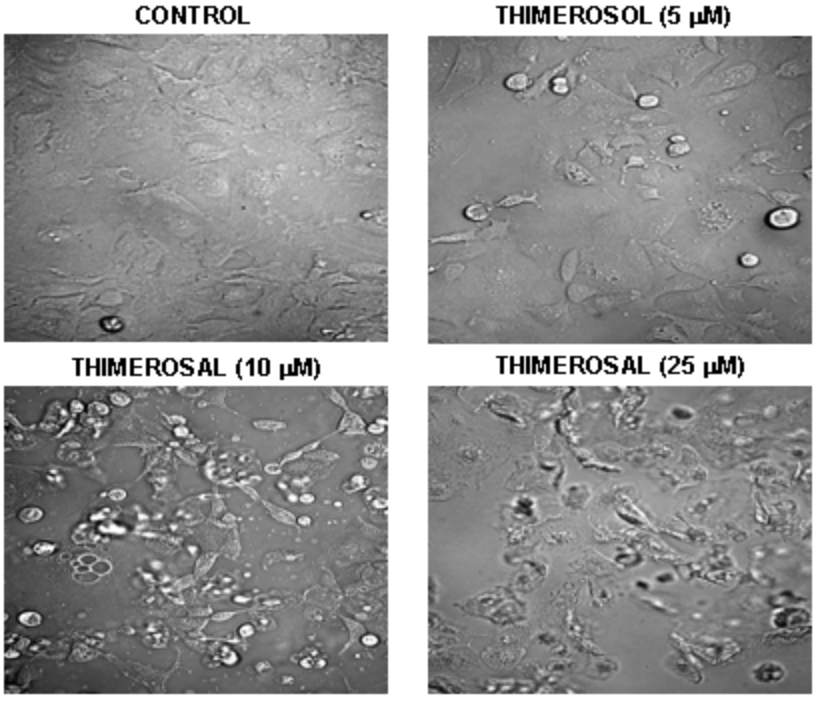

Figure 6

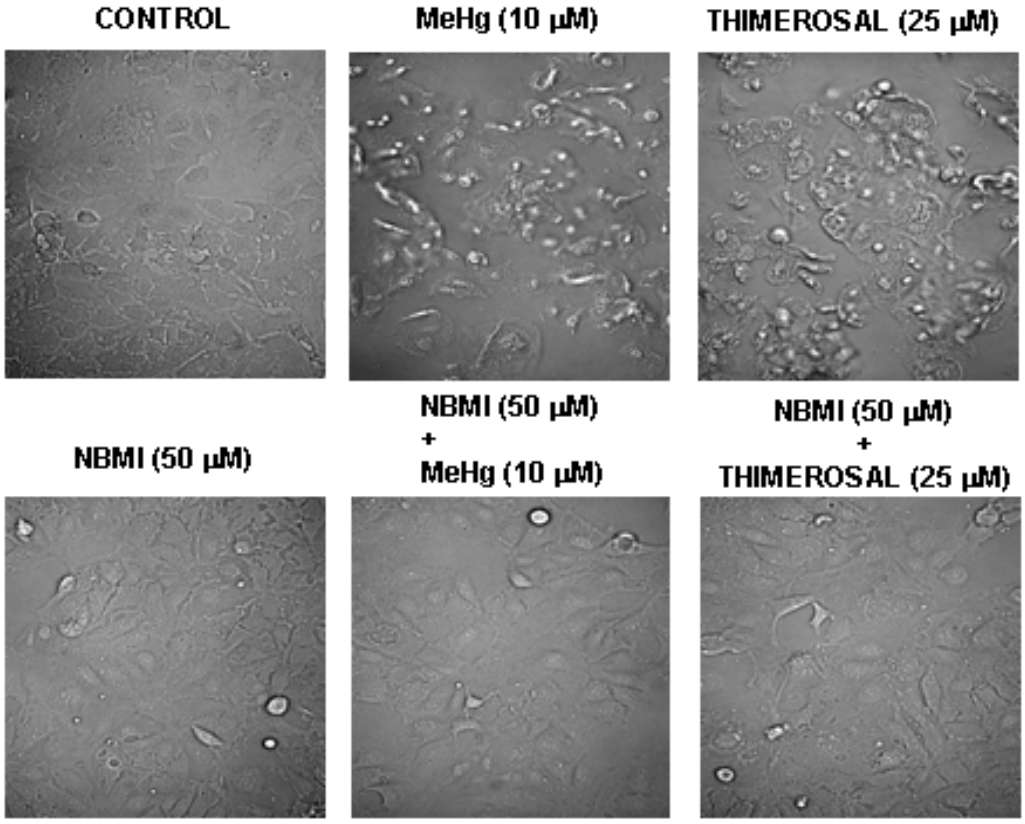
CONTROL
MeHg (10 µM)
THIMEROSAL (25 µM)
NBMI (50 µM)
NBMI (50 µM)
+
MeHg (10 µM)
NBMI (50 µM)
+
THIMEROSAL (25 µM)

Figure 7A

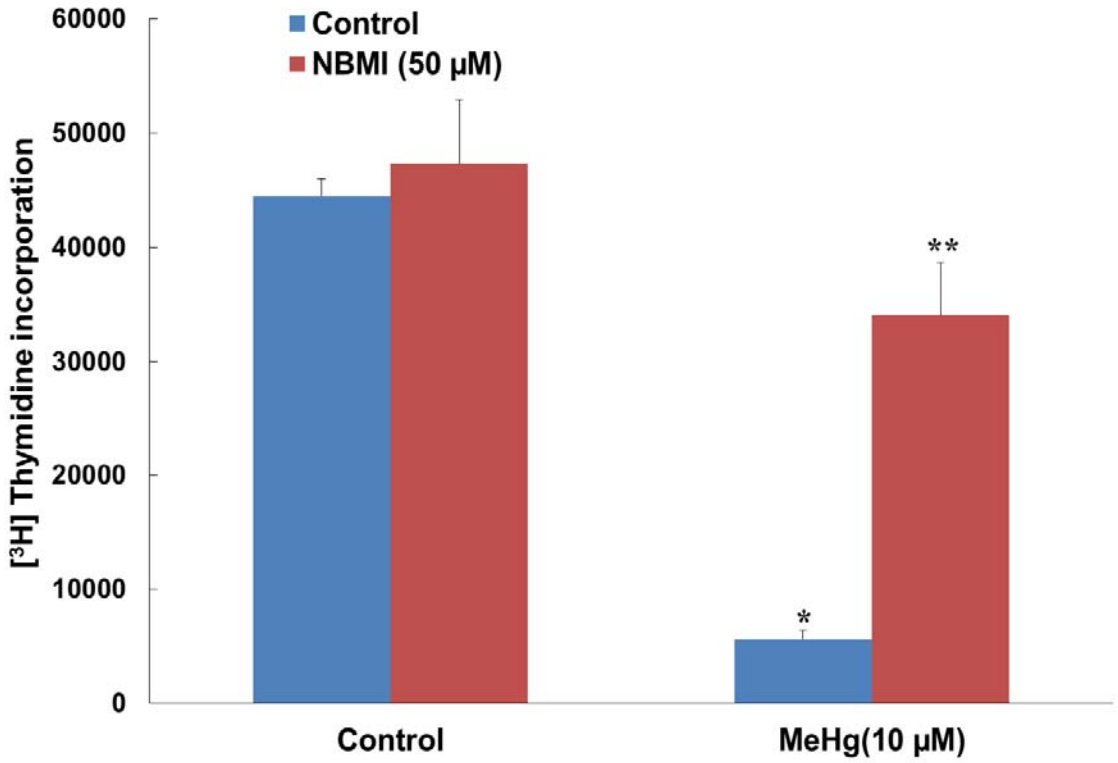

Figure 7B

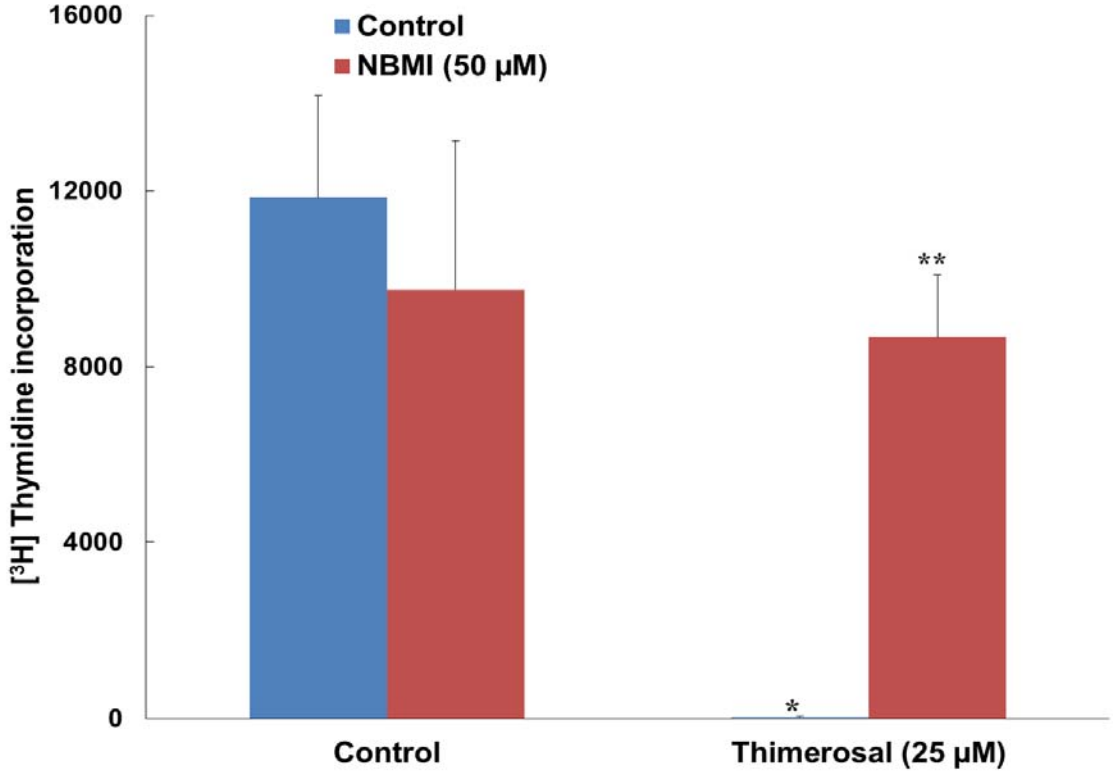

Figure 8A

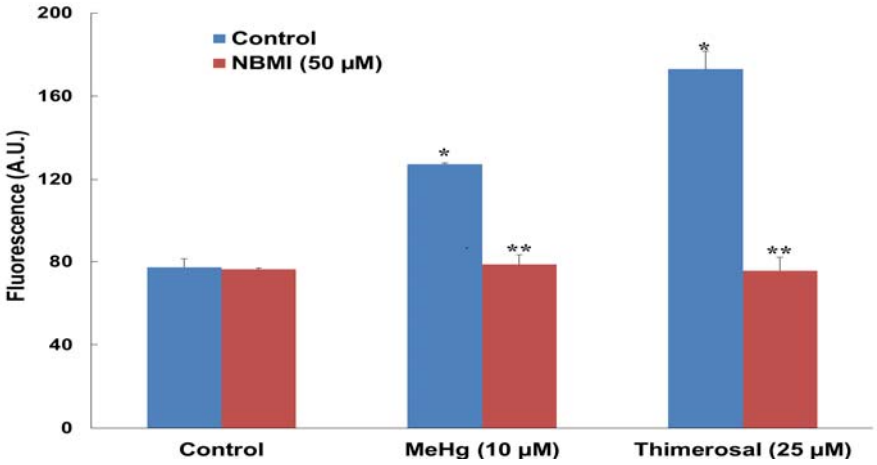

Figure 8B

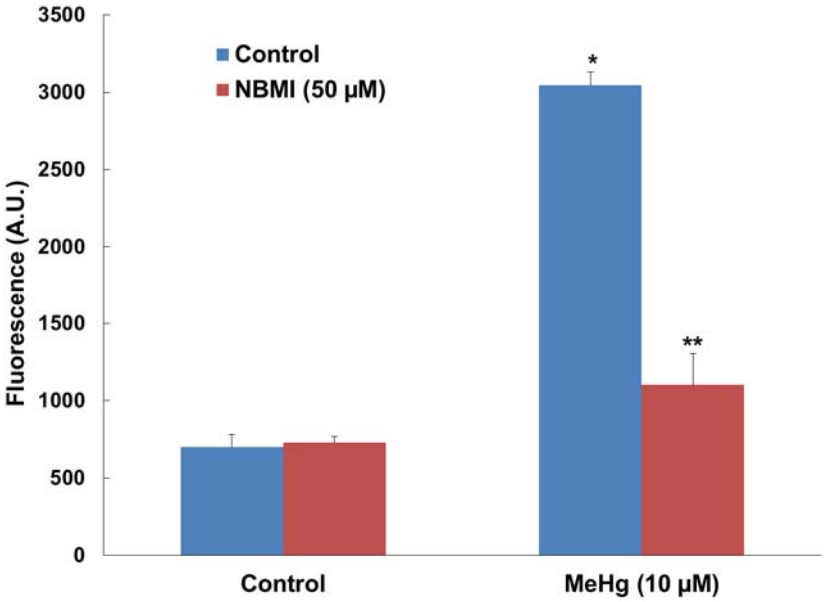

Figure 8C

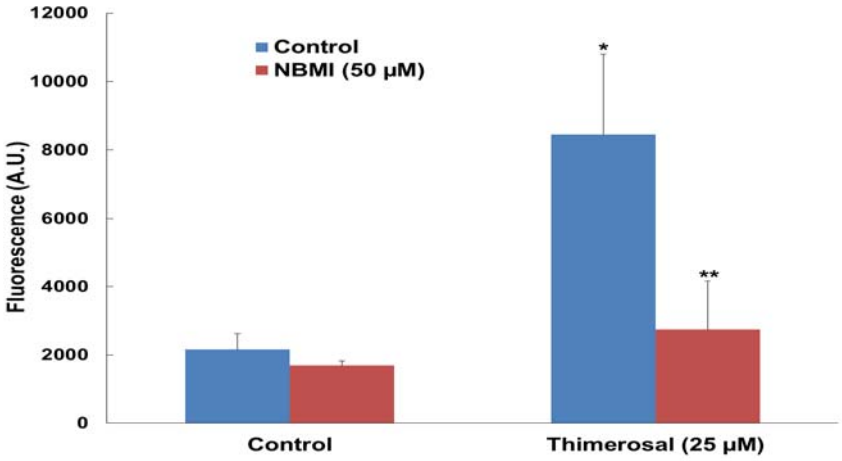

Figure 9

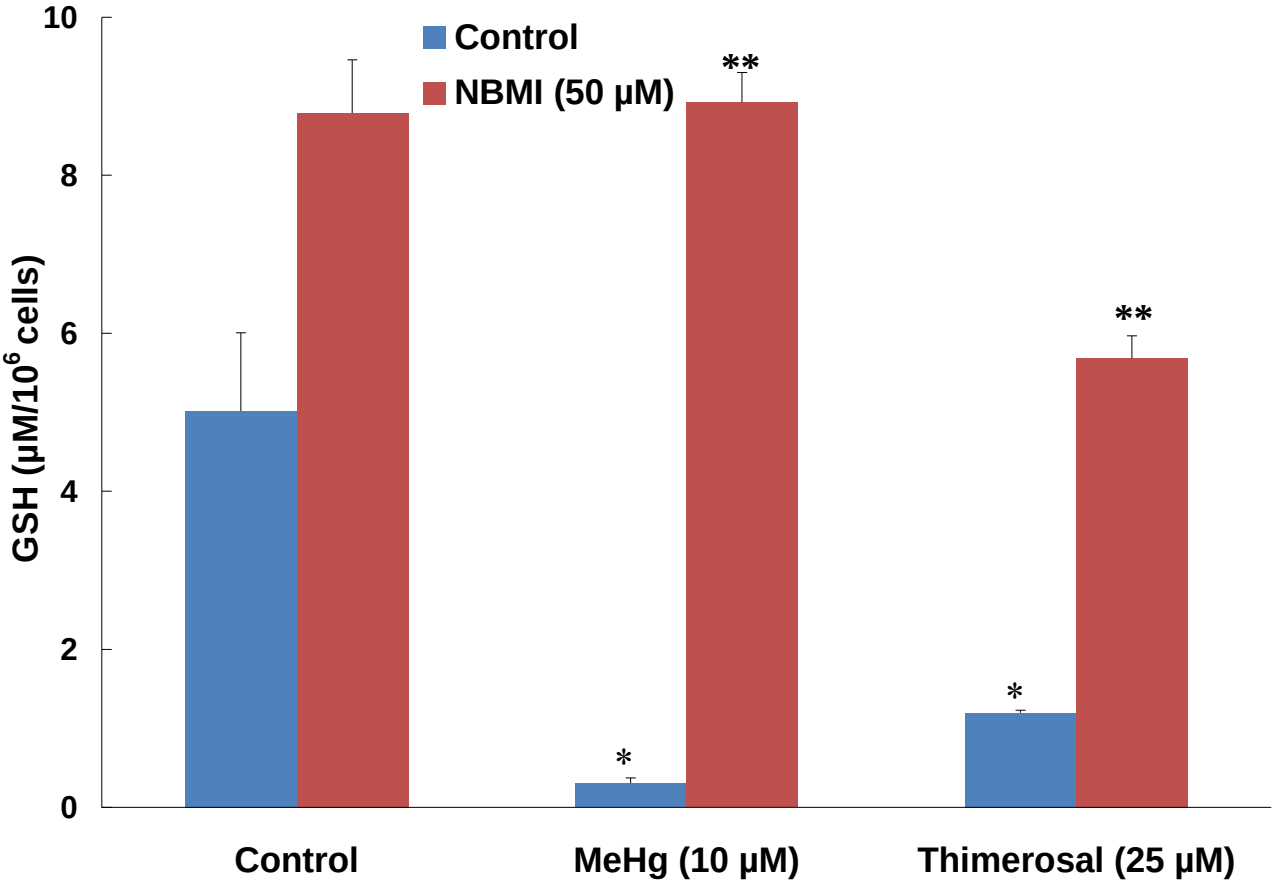
10
8
6
4
2
0
GSH (μM/10^6 cells)
Control
NBMI (50 μM)
**
*
**
*
Control
MeHg (10 μM)
Thimerosal (25 μM)

Figure 10A

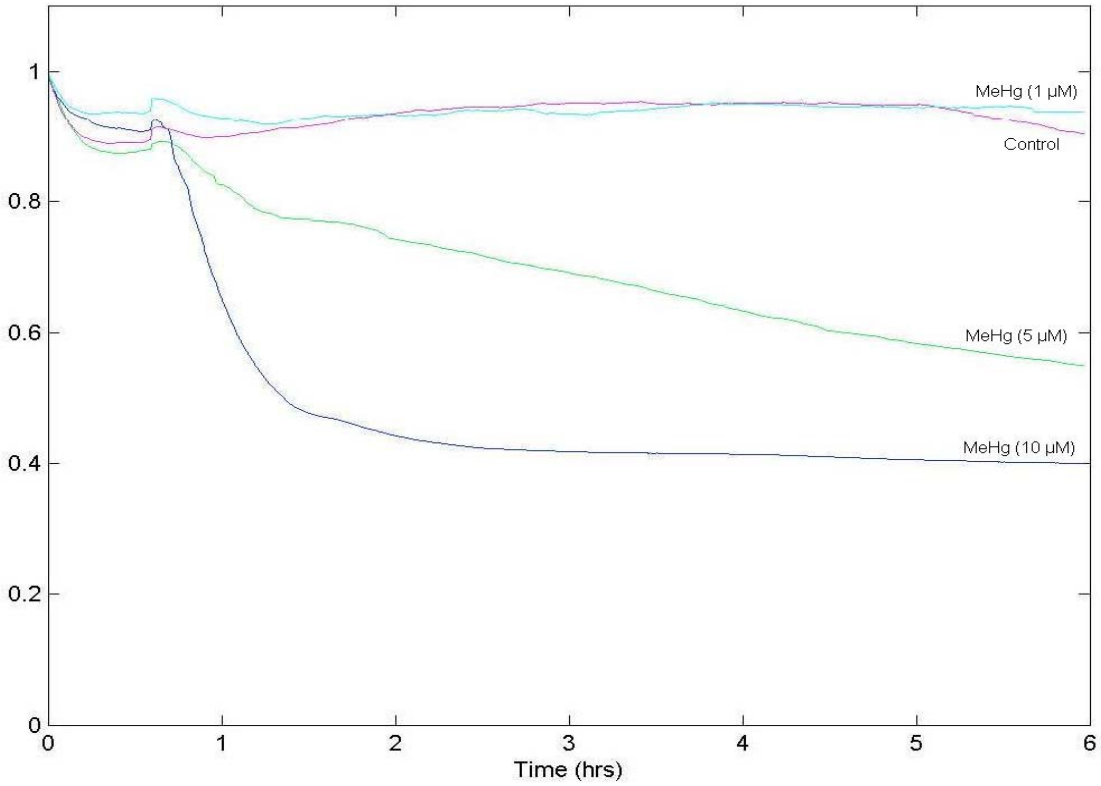

Figure 10B

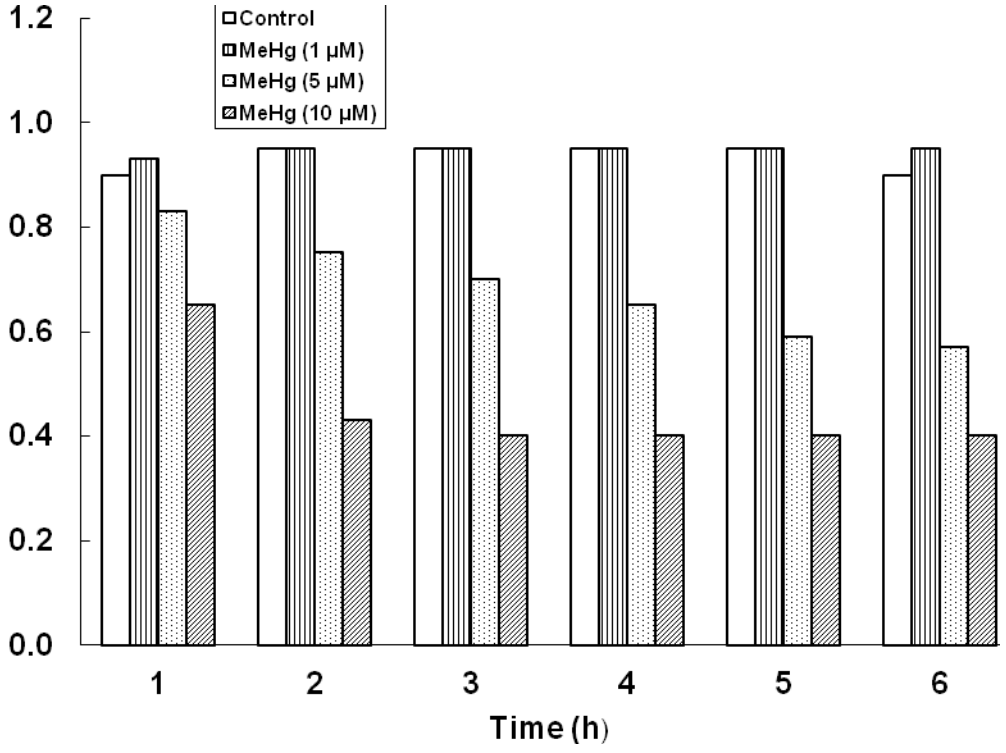

Figure 10C

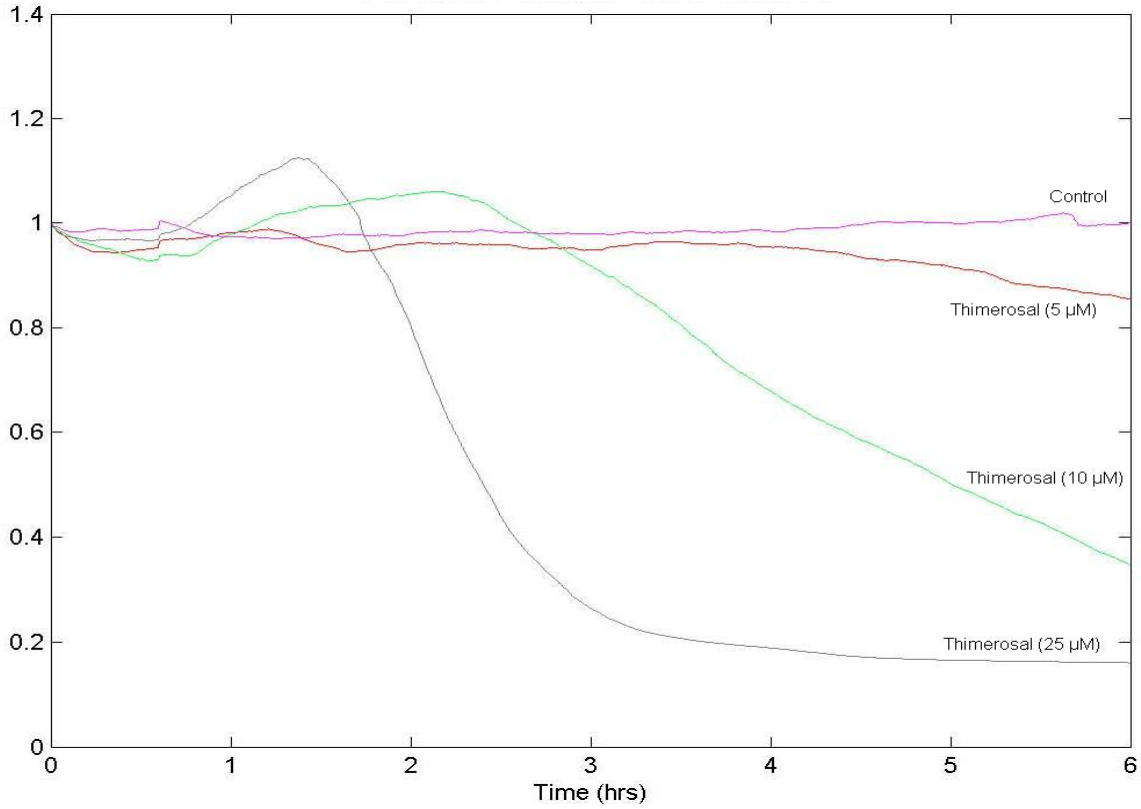

Figure 10D

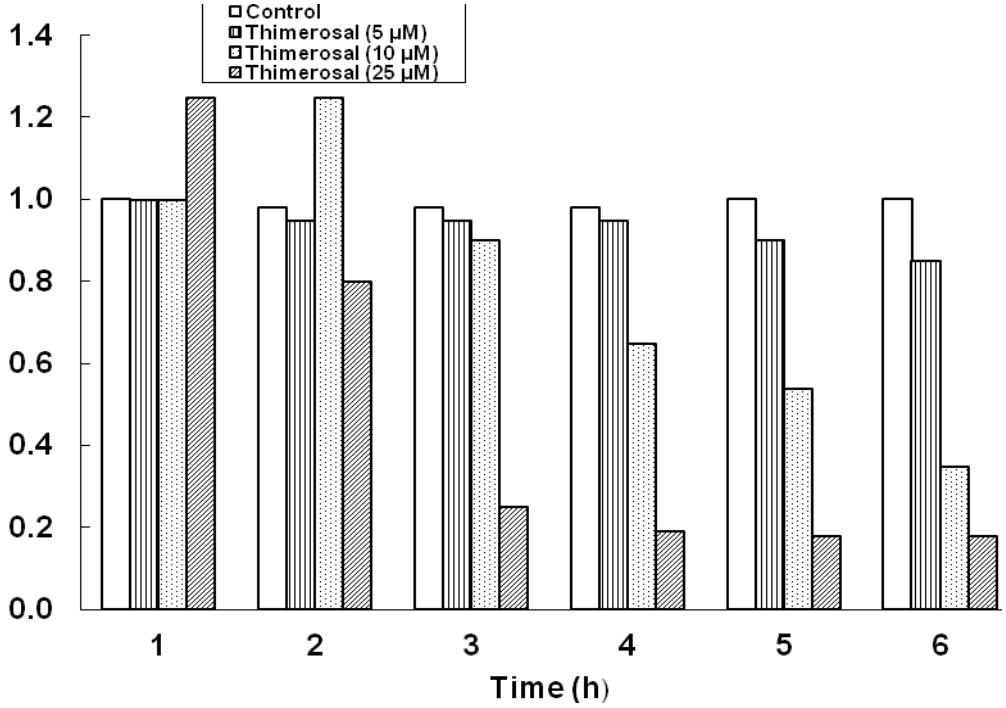

Figure 11A

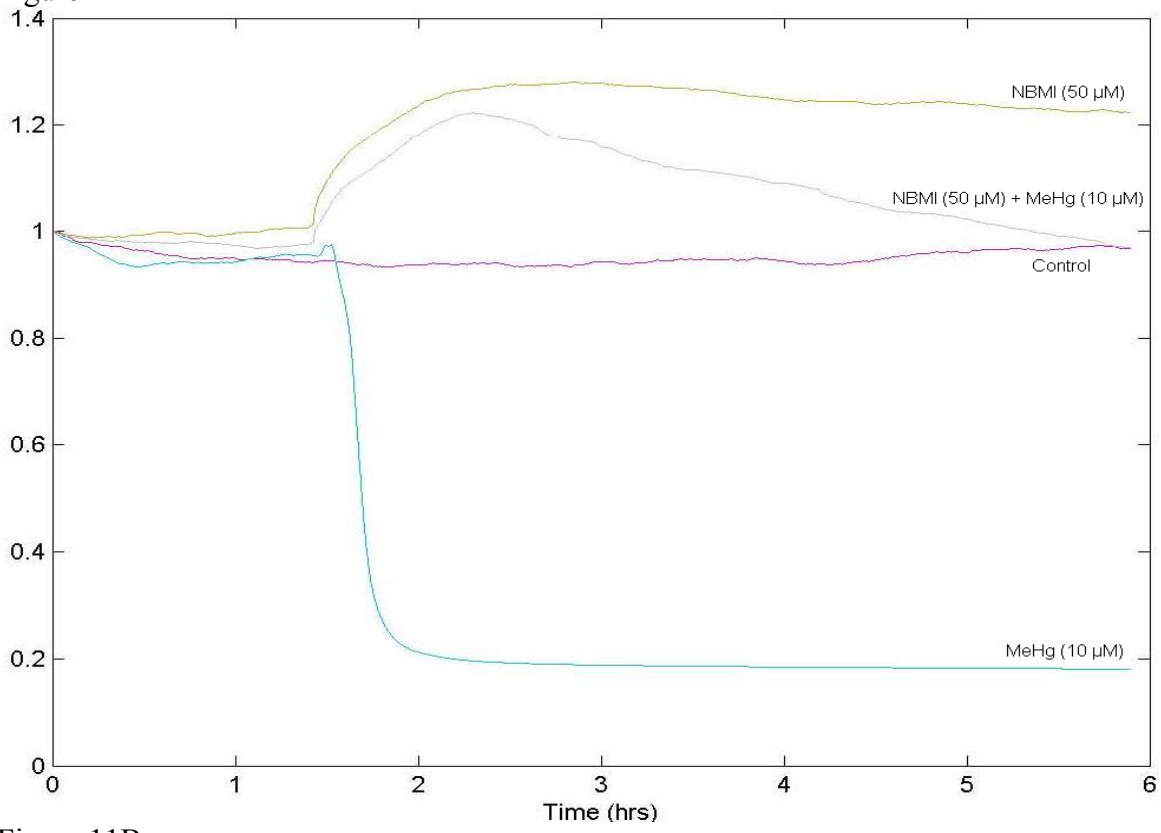

Figure 11B

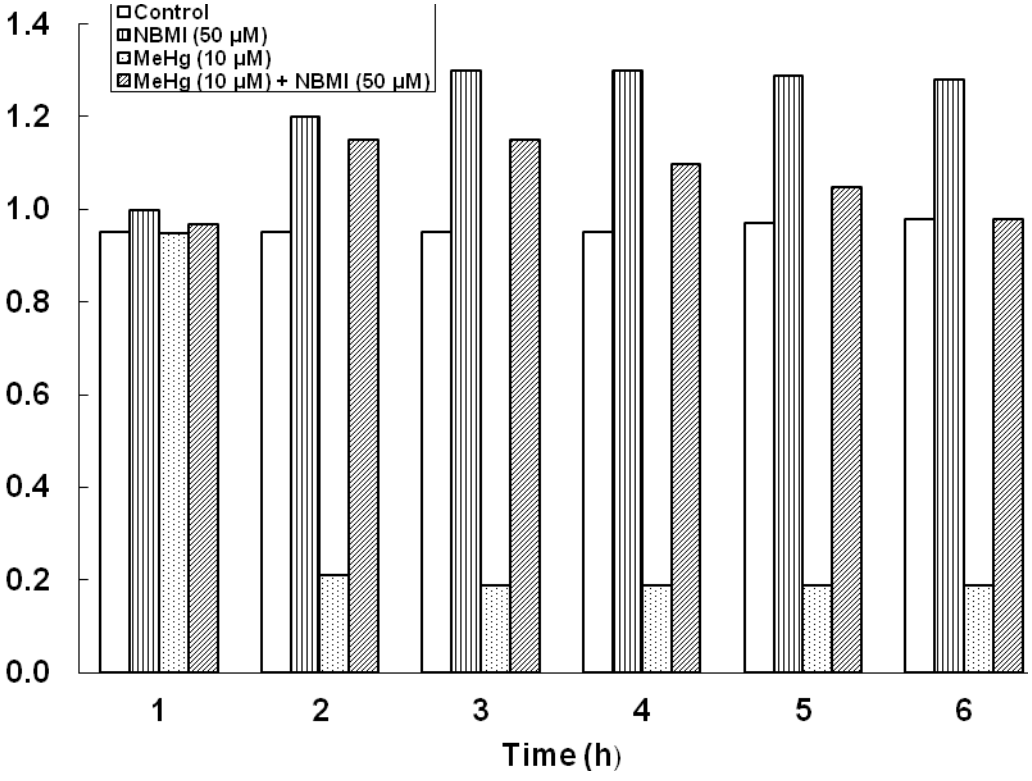

Figure 11C

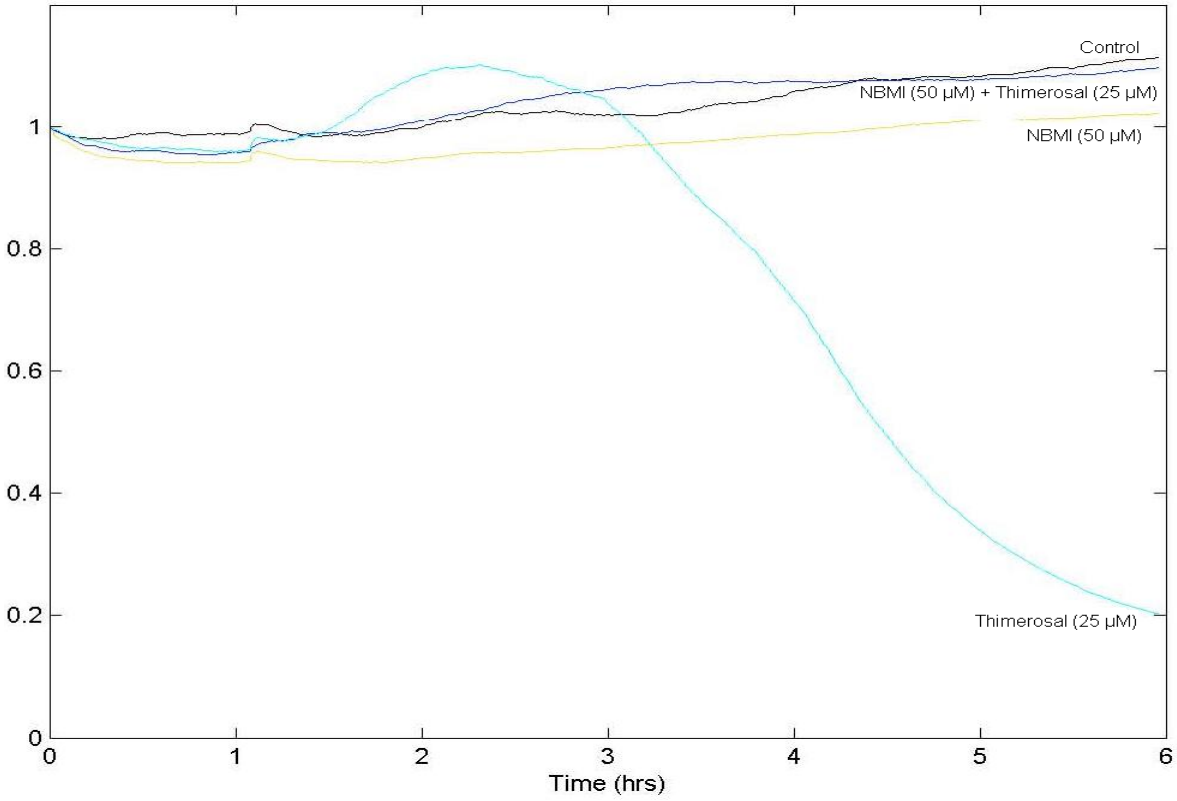

Figure 11D

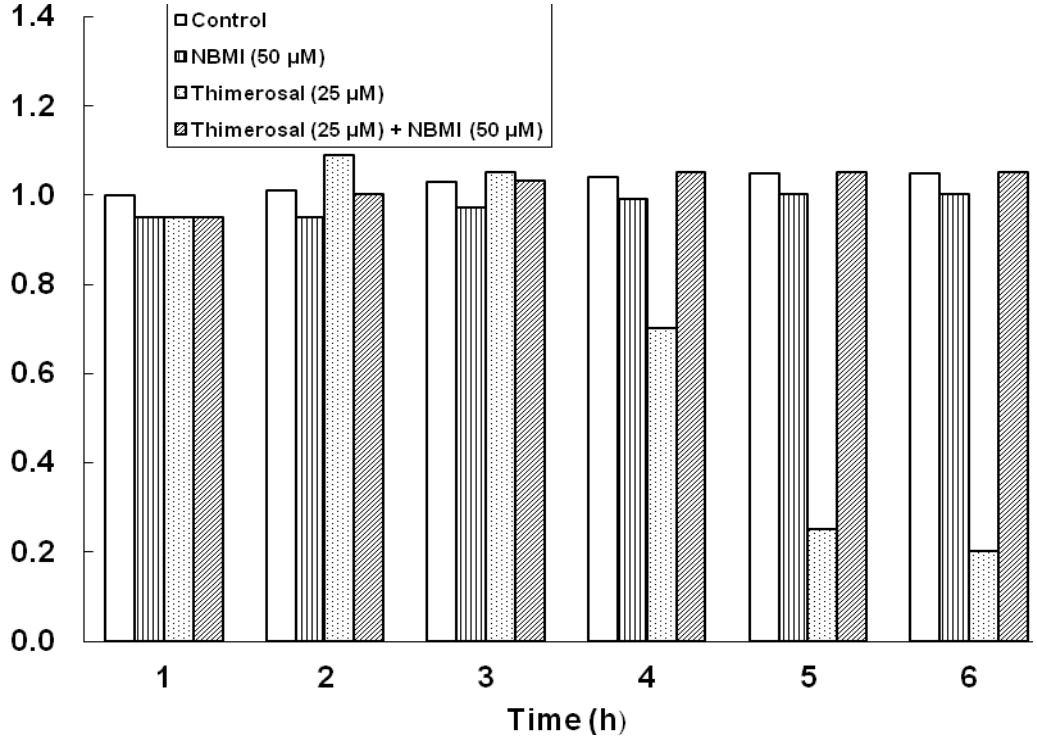

Figure 12

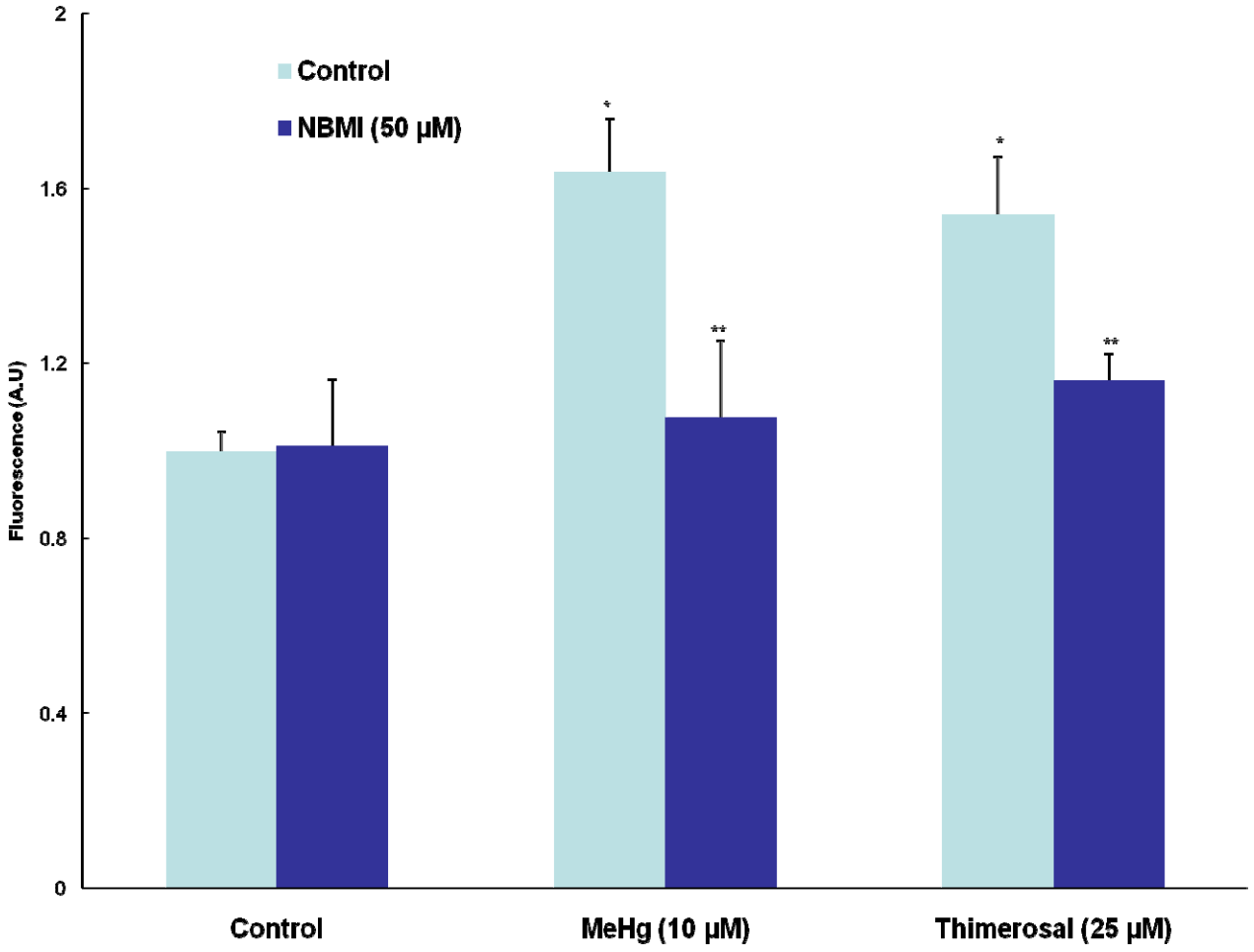
Control
NBMI (50 µM)
Fluorescence (A.U)
2
1.6
1.2
0.8
0.4
0
*
**
*
**
Control
MeHg (10 µM)
Thimerosal (25 µM)

Figure 13A

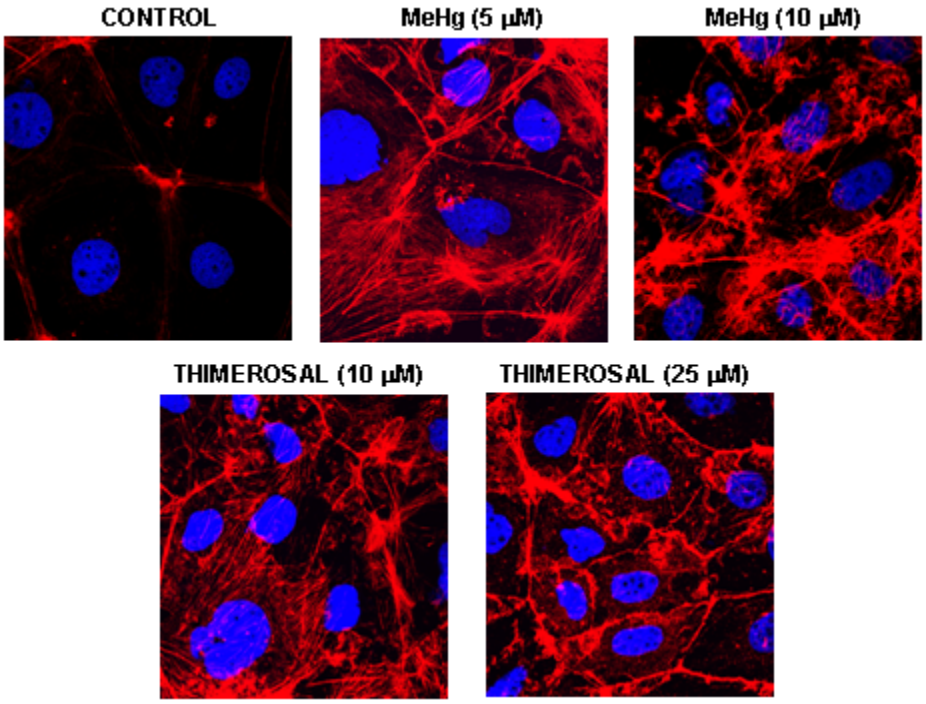

Figure 13B

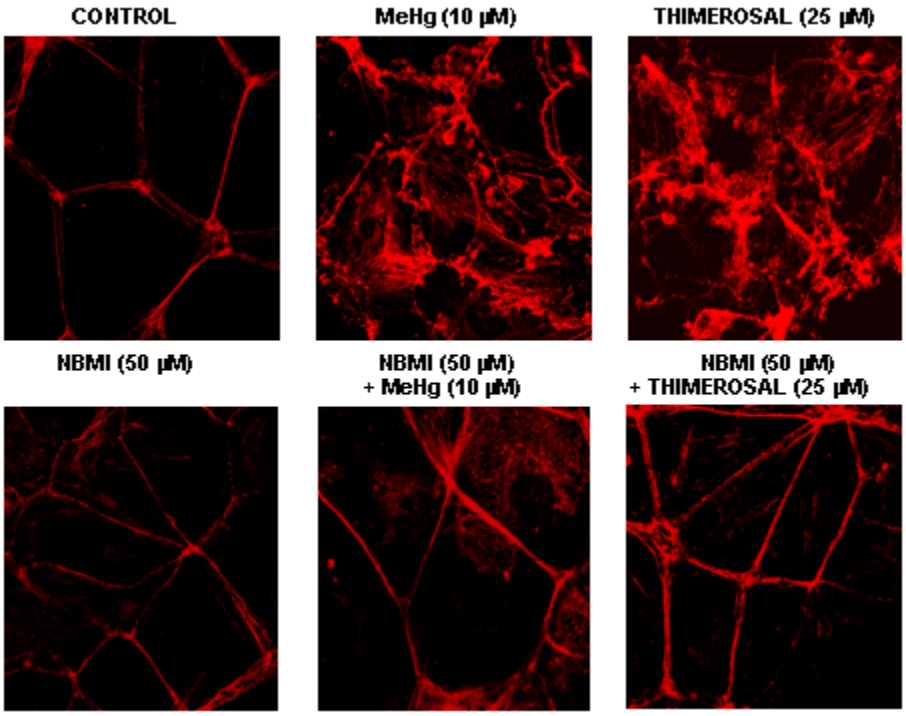

Figure 14A

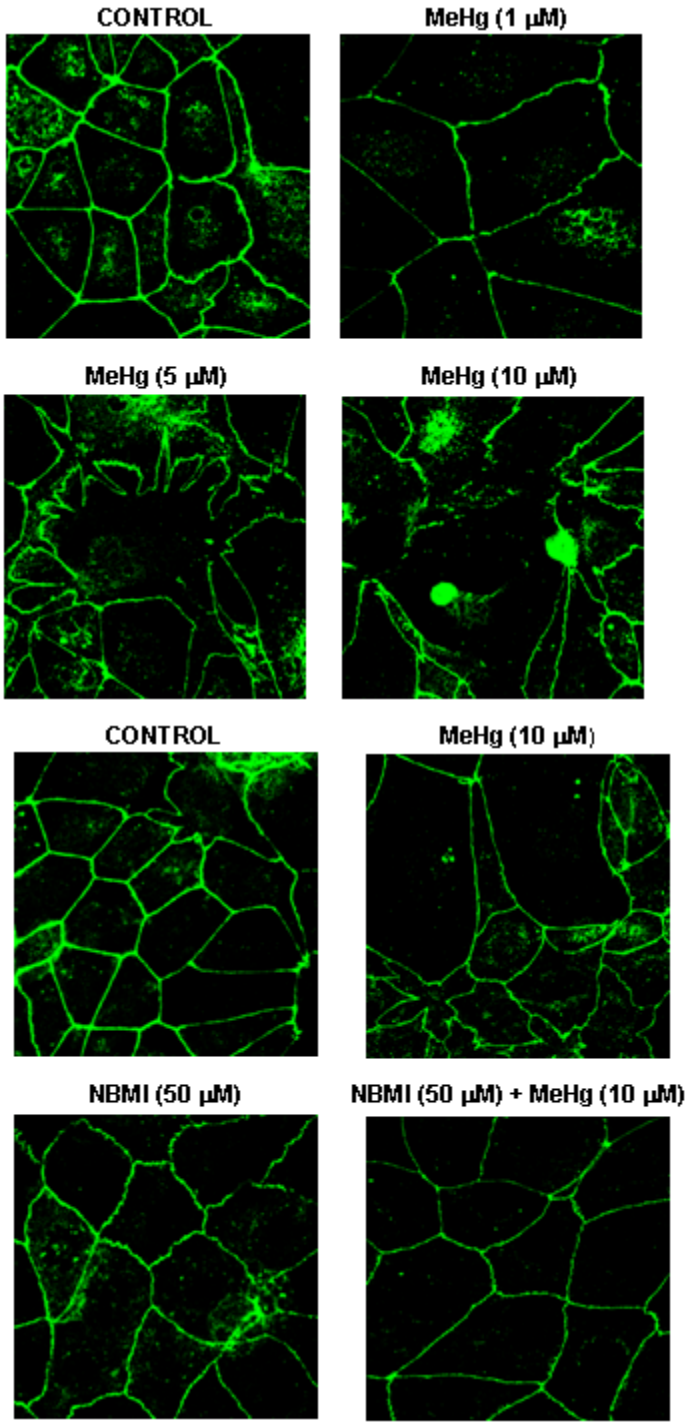
CONTROL
MeHg (1 µM)
MeHg (5 µM)
MeHg (10 µM)
CONTROL
MeHg (10 µM)
NBMI (50 µM)
NBMI (50 µM) + MeHg (10 µM)

Figure 14B

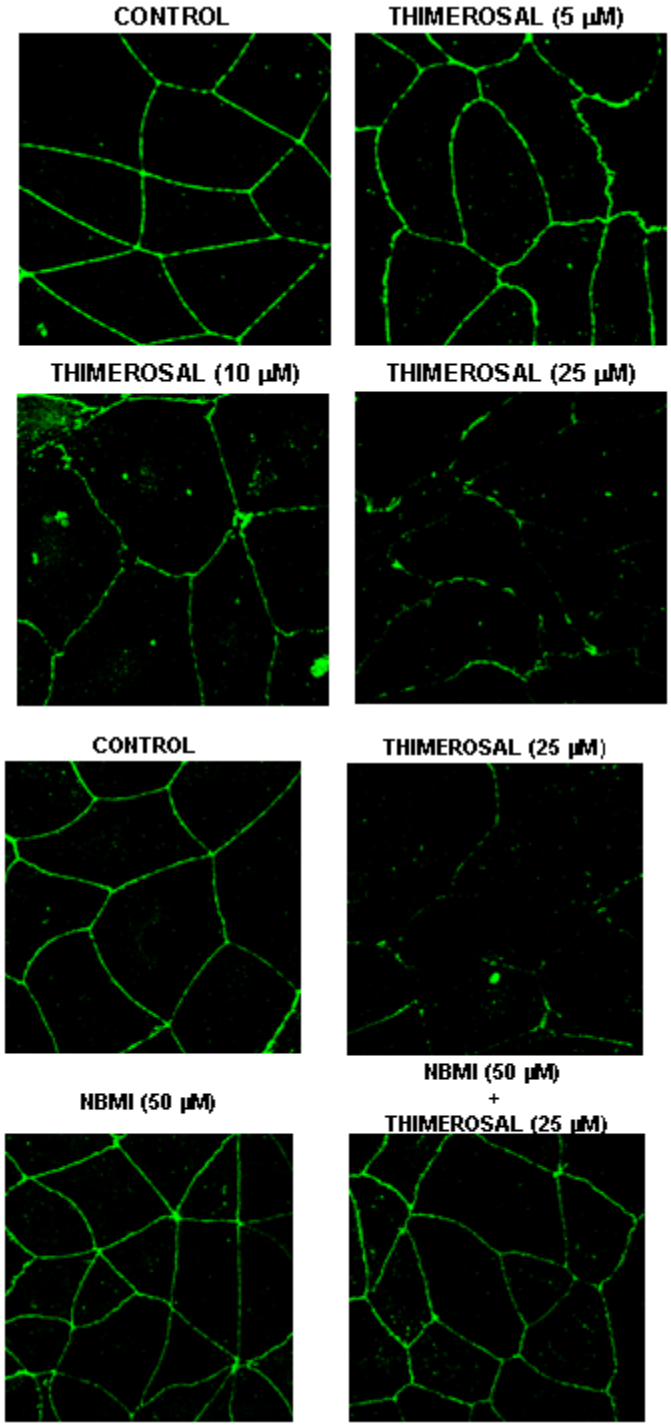
CONTROL
THIMEROSAL (5 µM)
THIMEROSAL (10 µM)
THIMEROSAL (25 µM)
CONTROL
THIMEROSAL (25 µM)
NBMI (50 µM)
NBMI (50 µM)
+
THIMEROSAL (25 µM)

Figure 14C

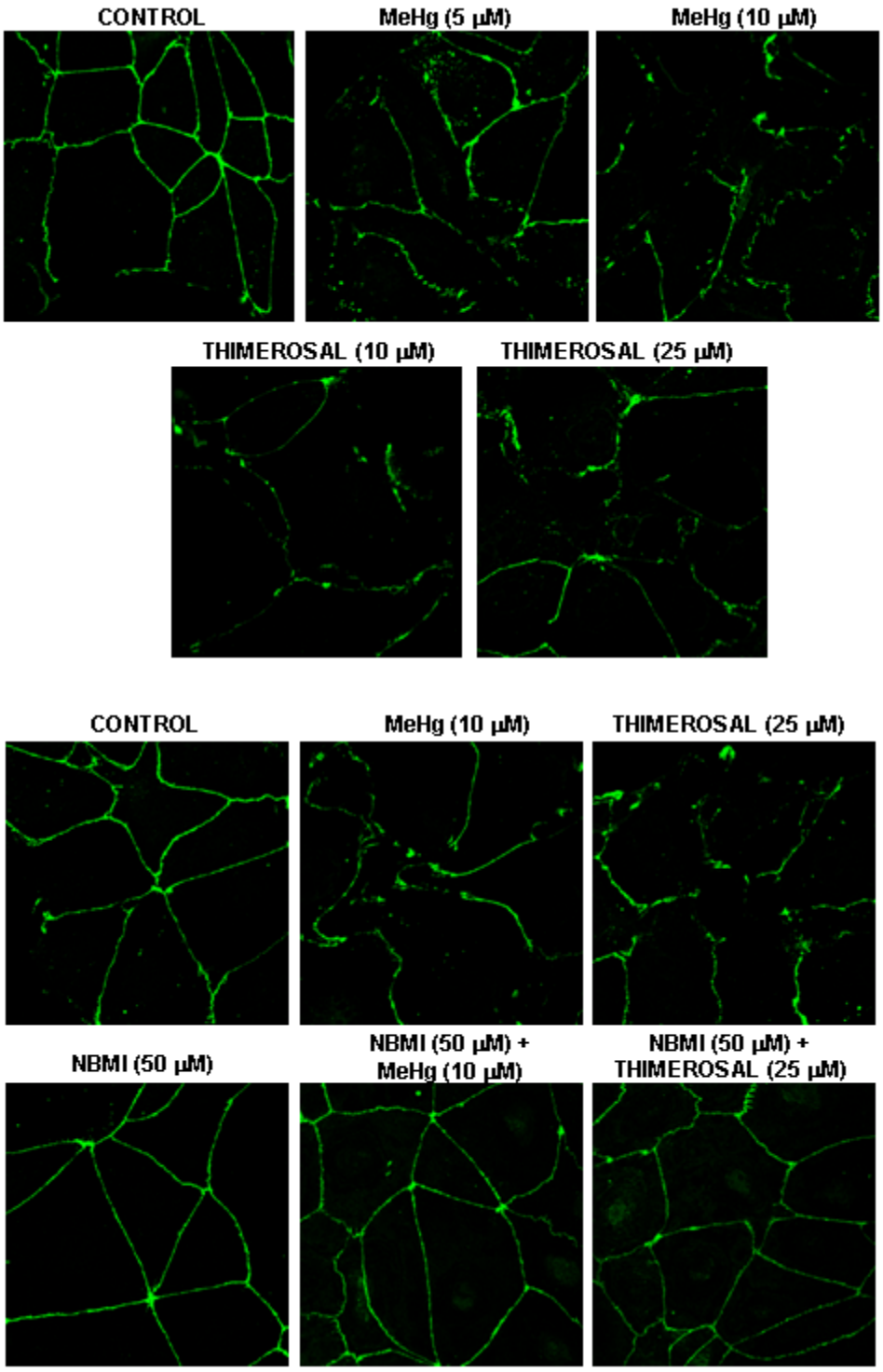
CONTROL
MeHg (5 µM)
MeHg (10 µM)
THIMEROSAL (10 µM)
THIMEROSAL (25 µM)
CONTROL
MeHg (10 µM)
THIMEROSAL (25 µM)
NBMI (50 µM)
NBMI (50 µM) + MeHg (10 µM)
NBMI (50 µM) + THIMEROSAL (25 µM)

Schema 1

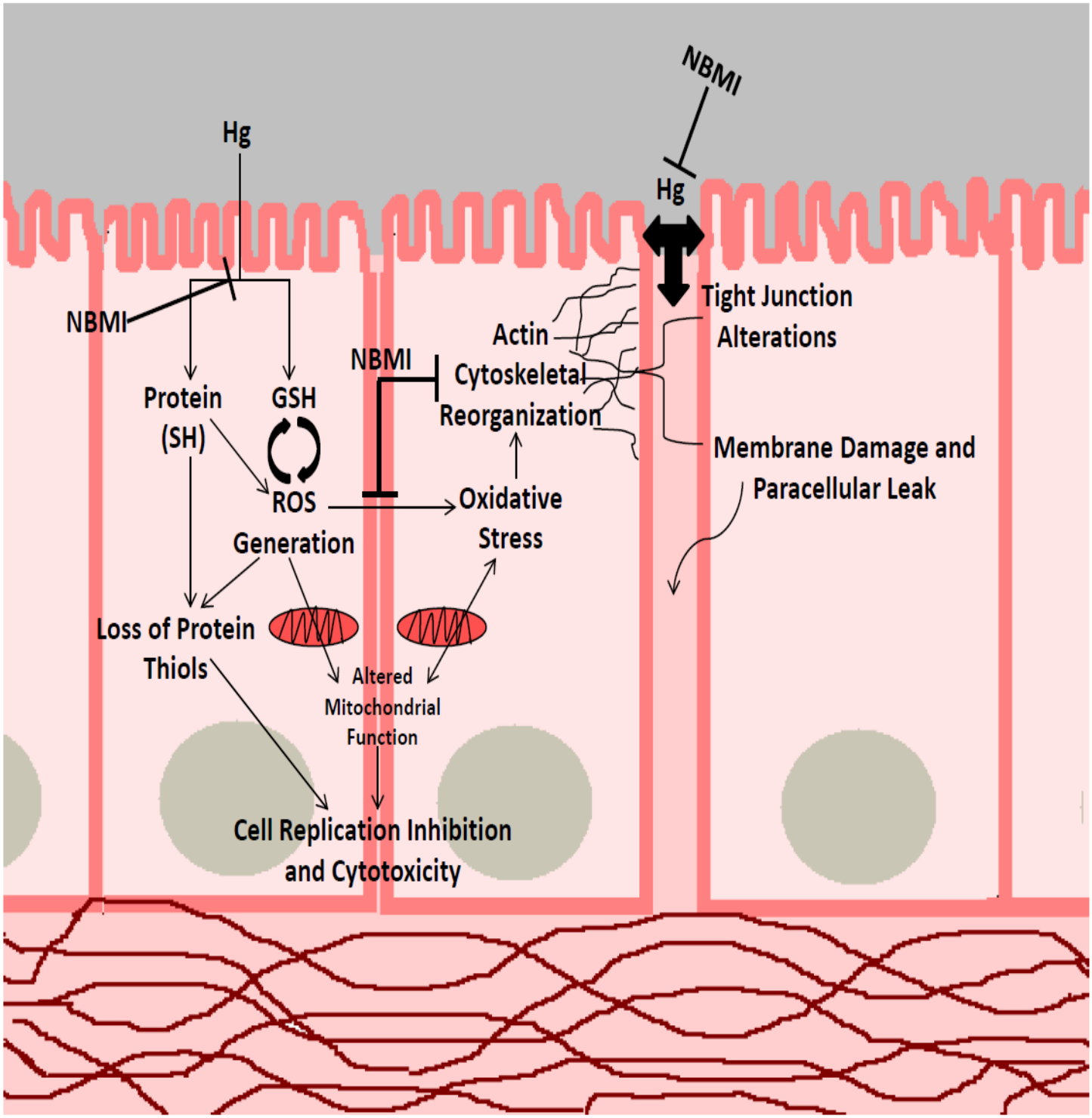
NBMI
Hg
Hg
NBMI
Tight Junction
Alterations
Actin
Cytoskeletal
Reorganization
NBMI
Protein
(SH)
GSH
ROS
Oxidative
Stress
Generation
Membrane Damage and
Paracellular Leak
Loss of Protein
Thiols
Altered
Mitochondrial
Function
Cell Replication Inhibition
and Cytotoxicity